

Accepted Manuscript

Design, synthesis, biological evaluation and molecular docking study on
peptidomimetic analogues of XK469

Qiao-Hong Xia, Wei Hu, Chen Li, Ji-Feng Wu, Liang Yang, Xue-Mei Han, Yue-Mao
Shen, Zhi-Yu Li, Xun Li



PII: S0223-5234(16)30653-5

DOI: [10.1016/j.ejmech.2016.08.010](https://doi.org/10.1016/j.ejmech.2016.08.010)

Reference: EJMECH 8806

To appear in: *European Journal of Medicinal Chemistry*

Received Date: 19 May 2016

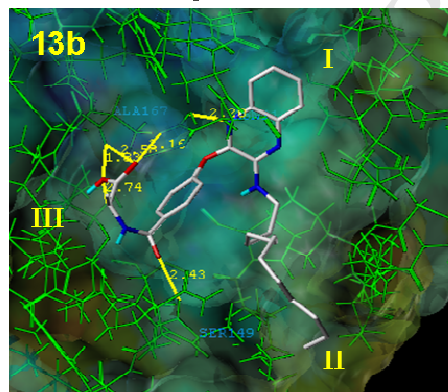
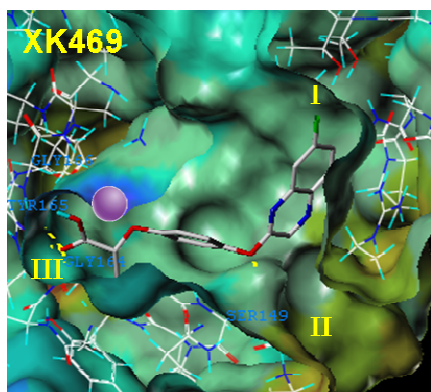
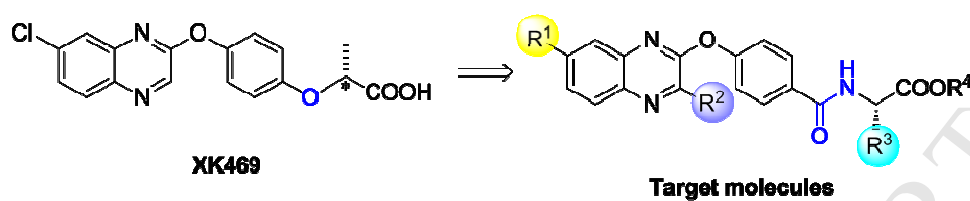
Revised Date: 5 August 2016

Accepted Date: 6 August 2016

Please cite this article as: Q.-H. Xia, W. Hu, C. Li, J.-F. Wu, L. Yang, X.-M. Han, Y.-M. Shen, Z.-Y. Li, X. Li, Design, synthesis, biological evaluation and molecular docking study on peptidomimetic analogues of XK469, *European Journal of Medicinal Chemistry* (2016), doi: 10.1016/j.ejmech.2016.08.010.

This is a PDF file of an unedited manuscript that has been accepted for publication. As a service to our customers we are providing this early version of the manuscript. The manuscript will undergo copyediting, typesetting, and review of the resulting proof before it is published in its final form. Please note that during the production process errors may be discovered which could affect the content, and all legal disclaimers that apply to the journal pertain.

Graphical abstracts



Design, synthesis, biological evaluation and molecular docking study on peptidomimetic analogues of XK469

Qiao-Hong Xia^{1,#}, Wei Hu^{2,#}, Chen Li³, Ji-Feng Wu⁴, Liang Yang¹, Xue-Mei Han¹, Yue-Mao Shen¹,
Zhi-Yu Li^{5,*}, Xun Li^{1,**}

¹ Department of Medicinal Chemistry, Key Laboratory of Chemistry and Chemical Biology (Ministry of Education),
School of Pharmaceutical Sciences, Shandong University, Ji'nan, Shandong 250012, P.R. China

² State Key Laboratory of Microbial Technology, School of Life Science, Shandong University, Ji'nan, Shandong
250100, P.R. China

³ School of Bethune Medical Sciences, Jilin University, Changchun, P. R. China

⁴ Institute of Criminal Science and Technology, Ji'nan Public Security Bureau, Ji'nan, 250100, P. R. China

⁵ Department of Pharmaceutical Sciences, Philadelphia College of Pharmacy, Philadelphia, PA, 19104, USA

Abstract

XK469 is identified as a potent quinoxaline antineoplastic agent based on its significant clinical efficacy. It probably exerts its activity *via* DNA topoisomerase II (topo II) inhibition. To obtain more effective antineoplastic agents, a spectrum of peptidomimetic-type quinoxaline analogues of XK469 was herein designed, synthesized, and evaluated. Few compounds (*e.g.* **13a** and **13b**) exhibited obvious cytotoxicity indicated by *in vitro* anti-proliferative assay. SAR investigation revealed that introducing of hydrophobic *tert*-butylamine or dodecylamine moiety at the 3-position of quinoxaline core is favorable for achieving a better anti-proliferative potency, while peptidomimetic derivatives only yielded moderate cytotoxicity. Compounds with improved anti-proliferative activities also demonstrated decent anti-metastatic potencies comparable with that of doxorubicin (Doxo) based on *in vivo* mouse model study. The topo II-mediated kinetoplast DNA (*kDNA*) decatenation assay as well as molecular docking studies implicated that these compounds tend to be potent topo II inhibitors. Overall, compounds **13a** and **13b**, **13b** in particular, stood out from various assessments and might be promising candidates for further chemical optimization.

Keywords: XK469; quinoxaline peptidomimetic analogues; hydrophobic chain; topoisomerase II inhibitor; antineoplastic agents.

[#]These two authors contributed equally to this manuscript. ^{*}Corresponding addresses at:

^{*}Zh.Li@uscience.edu; ^{**}tjlx2004@sdu.edu.cn (Li. X)

1. Introduction

Almost all anticancer chemotherapeutics exert their therapeutic efficacies by killing fast dividing cells and cause severe side effects. Cancer cells also quickly develop multidrug resistance (MDR) through different mechanisms. The synthetic quinoxaline derivative XK469 (NSC 697887), or (±)-2-[4-(7-chloro-2-quinoxalinyloxy)phenoxy]propionic acid, is a promising lead compound, due to its significant therapeutic efficacy against a broad spectrum of solid tumors and high activity towards numerous types of MDR cancers. More importantly, it exhibited relatively low toxicity and side effects, compared with many conventional antineoplastic agents, such as camptothecin [1, 2].

Despite its significant antitumor potency, the exact biotarget(s) and action mechanism of XK469 have not been clearly elucidated. At present, the proposed putative mechanisms are related to the induction of G₂-M cell cycle arrest by p53-dependent and -independent pathways [3], apoptosis regulation [4], MEK/MAPK signaling pathway [5], inhibition of cyclin B1 ubiquitination [6], or mixed autophagy [7]. Recently, more evidences have supported that XK469 is more likely to function as a selective topo II inhibitor, while has no or weak effect on topo I [8-10].

Sustained efforts from Horwitz's group have clearly elaborated the structure-activity relationship (SAR) of XK469 [11-15]. The parent structure of XK469 can be dissected into three parts (Fig. 1): quinoxaline core (part A), hydroquinone linker (part B), and the lactic acid portion (part C). For part A, the bicyclic quinoxaline framework generated the highest activity, while replacement of quinoxaline frame with other rigid cyclic structures, in contrast, would lead to considerably decreased potency. As far as the impact of substitution on quinoxaline ring was concerned, the 7-halogen substitution eventually gave the best potency, with an activity order of F \approx Cl \approx Br > I, followed by compounds without any substituent at this site. Other substituents, such as methyl, methoxyl, nitro, amino or azido, generated much less activities. When halogen was added to other sites, all derivatives were inactive against cancer cells. For part B, either a resorcinol or a catechol replacement resulted in the loss of antineoplastic activity, suggesting the hydroquinone connecting motif is essential for maintaining the antineoplastic potency. For part C, although R(+)- and S(-)-isomers have equal toxicity in animal tumor models, R(+) stereoisomer (NSC 698215) is slightly more potent than S(-)-isomer (NSC 698216) [8]. Moreover, when carboxylic acid was replaced by other groups, such as CONH₂, CONHCH₃, CON(CH₃)₂, CONHOH, CONHNH₂, CN, or CN₄H (tetrazole), the corresponding derivatives displayed impaired antineoplastic activities, compared with that of free acid counterparts. Only when carboxylic acid was converted into carboxylic ester or *N,N*-dimethylamide motif, these derivatives exhibited slightly decreased bioactivities, implying an intact 2-oxypropionic acid frame is a prerequisite for maintaining maximum antitumor potency as well as optimal water solubility. Collectively, based on the SAR analysis of XK469, we can draw a conclusion that the quinoxaline ring with 7-halogen substitution (or without substitution), hydroquinone mode, and R(+)-form 2-oxypropionic acid motif are favorable contributors for achieving a higher antineoplastic efficacy.

“Enhancing protein backbone-binding” concept has been validated as an effective mean to combat

drug resistance [16], which was thereby utilized in this work with an expectation of confronting MDR in cancer cells. According to the 3D structure of topo II (PDB entry: 1ZXN), it clearly evinced that the protein backbone possesses three important binding domains, *via* pocket I, II and III, as evinced in Fig. 1. The binding pattern of XK469 with topo II revealed that the quinoxaline ring of XK469 (**part A**) locates in pocket I, a relatively wide hydrophobic area, and the 1-N of XK469 forms a H-bonding interaction with the lateral phenolic hydroxyl H of Tyr34, with a distance of 2.16Å. The polar carboxylic acid portion (**part C**) inserts into pocket III, and the hydroxyl O, as an H-bond acceptor, interacts with the skeletal NHs of Gly166 (2.58Å), Tyr165 (2.01Å) and Gly164 (1.82Å), respectively. In regard to the hydroquinone connecting motif (**part B**), although the adjacent O of quinoxaline core orients toward the pocket II by forming a H-bond with Ser149 (2.18Å), a hydrophobic side chain seems to be preferably introduced into this relatively narrow cavity, resulting in enhanced protein backbone-binding effect *via* the formation of effective hydrophobic interaction.

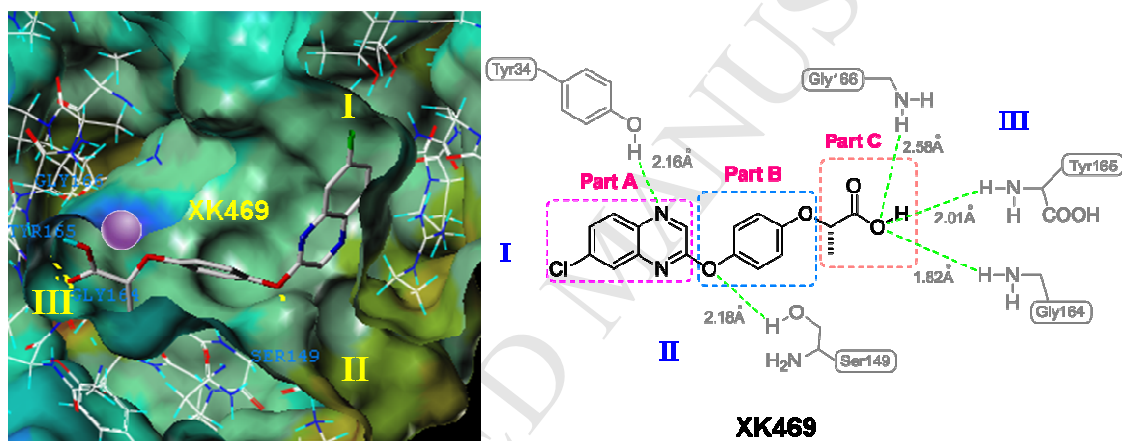


Fig. 1. Crystal structure of topo II (left) and binding mode of XK469 with topo II (right). H-bonding interactions are represented as dot lines.

Hydrophobic *tert*-butyl chain was initially selected since it has been frequently found in topo II inhibitor design. For instance, Kundu and co-workers have developed an array of 2-aryl-*N*-fused aminoimidazole derivatives as potent topo II inhibitors [17]. SAR exploration suggested the *tert*-butylamine group at the 3-position is crucial for retaining high affinity for topo II. Binding mode of the most potent inhibitor (compound **I**, Fig. 2) against the ATPase domain of human topo II α indicated that the substituted 3-*tert*-butyl group not only provided a hydrophobic interaction through occupying a hydrophobic pocket surrounded by Asn91, Asp94 and Arg98 residues, but participated in an additional CH \cdots O type contact with the side chains of Asp94 and Asn91. This weak H-bonding interaction was presumed to offer an extra stability and make a positive contribution to the association of protein-ligand adducts [18]. Moreover, other two *tert*-butyl-containing topo II inhibitors, quinoline aminopurine compound **II** [19] and ATP-competitive purine analogue **III** [20], as shown in Fig. 2, were also proved to fit well in the hydrophobic pocket and form effective hydrophobic contacts with surrounding amino acid

residues.

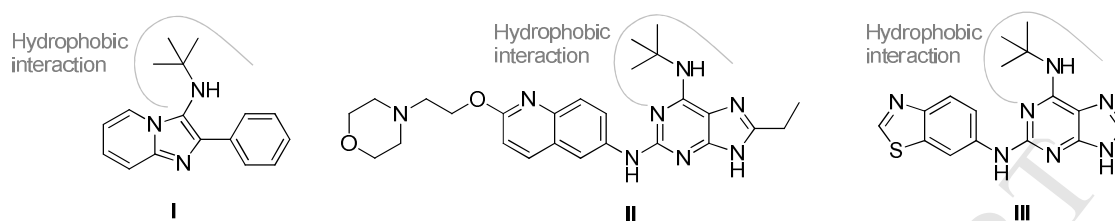


Fig. 2. Examples of topo II inhibitors that contain hydrophobic *tert*-butyl functional group.

Recently, long-chain fatty acids (LCFAs), including dodecanoic acid (lauric acid), octadecanoic acid, arachidic acid, *etc.*, have emerged as powerful tools for constructing efficient drug delivery system in conjunction with albumins [21-24]. Accordingly, LCFA carrier, such as human serum albumin (HSA) [22, 24], may efficiently deliver LCFA-conjugated antitumor drugs to tumor sites where payloads can be released and exert their bioactivities, and achieve preferred pharmacokinetic profiles as well [25, 26]. In addition, LCFAs are normally highly accumulated in cancer cells, in which LCFAs may not only serve as a crucial energy resource for cell growth, but furnish essential substances for rapid proliferation, development, and invasion [27, 28]. Therefore, LCFA chain is also chosen to fit the pocket II for enhanced topo II binding affinity as well as albumin-mediated drug delivery and formulation.

Based on the above SAR analysis and also as a long-standing interest in engaging in the research of peptidomimetic-derived medicinal chemistry [29-38], we hereby aimed to exploit a novel series of quinoxaline analogues of XK469 by incorporating these useful pharmacophoric groups and antitumor inducements (*e.g.*, *tert*-butyl and LCFA moieties) into a single peptidomimetic molecule for achieving potent antineoplastic activity. Specifically, the design concepts of these novel XK469 analogues are described as followings (Fig. 3): (i) The quinoxaline backbone (**part A**) is kept, and Cl and H atoms are selected as R¹ substituent at the 7-position. To better understand how the disposition of substituents on the quinoxaline core affect the bioactivity, substitution at the 6-position was also explored; (ii) The R² group at the 3-position is attached with hydrophobic methyl, *tert*-butylamine, or dodecylamine fragments, aiming to acquiring both effective hydrophobic contacts and possible enhanced affinity by penetrating into pocket II of topo II. Besides, the basic amine motif in these substitutions is also believed to benefit the drug uptake of cancer cells [39]; (iii) The essential hydroquinone connecting part (**part B**) remains unchanged, and the naturally available L-propionic acid is directly incorporated to construct the R(+) free acid portion (**part C**), with an intention to avoid chiral synthesis or separation, and thus simplifying the synthetic procedures. More importantly, the amino group of incorporated L-propionic acid can readily react with another carboxylic acid to build a desirable peptidomimetic function. As a surrogate for the O atom of XK469, the integrated amide bond might produce better binding affinity for biotarget through offering potential H-bonding donor (NH) and acceptor (C=O), and subsequently gain an elevated activity. Additionally, to further expand the SAR investigation as well as biological scope of quinoxaline peptidomimetic derivatives, we have explored the chemical diversification by introducing other L-amino acids (*e.g.* leucine,

phenylalanine, isoleucine, glycine), in addition to alanine.

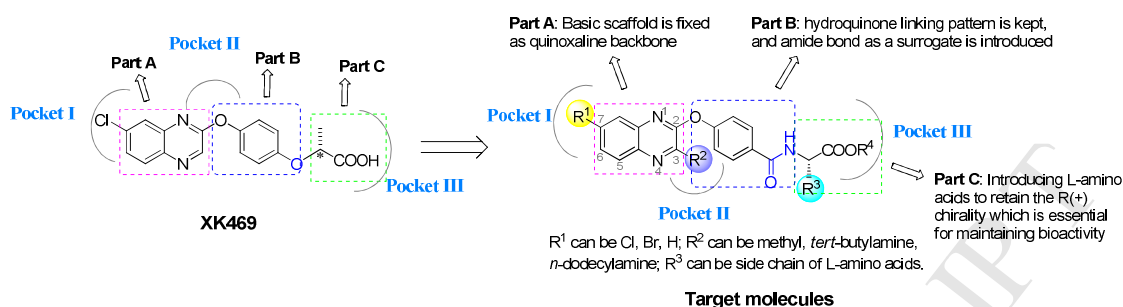


Fig. 3. The design concepts of quinoxaline peptidomimetic analogues of XK469.

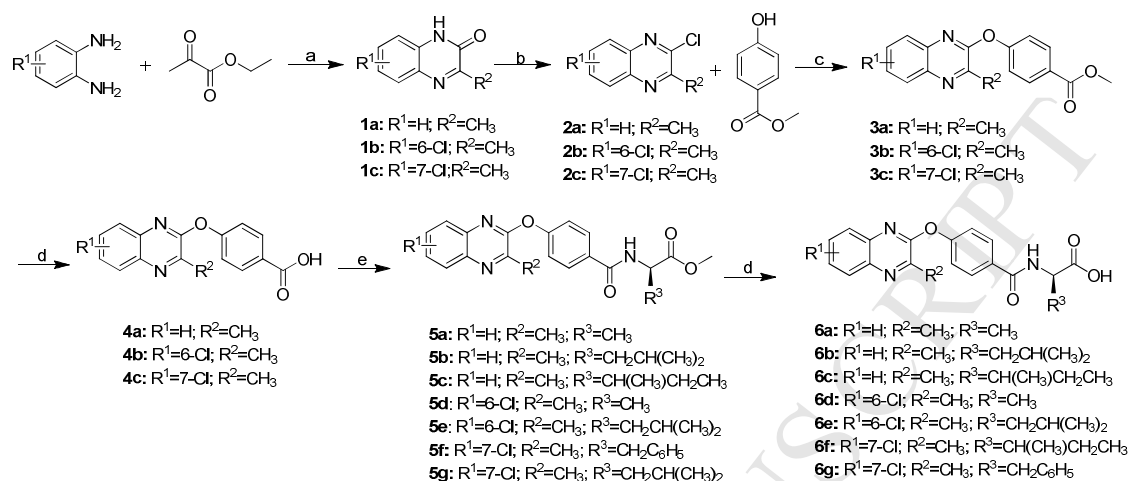
To test the above assumption, a spectrum of quinoxaline peptidomimetics were synthesized, and *in vitro* and *in vivo* antitumor activities were consequently evaluated. Moreover, preliminary SAR investigation, mechanism of action, and molecular modeling study of these derivatives were also examined. All together, we hoped the present exploration on the XK469 analogues might provide a clue for further development of diversified peptidomimetic derivatives with antineoplastic potentials.

2. Results and discussion

2.1. Chemistry

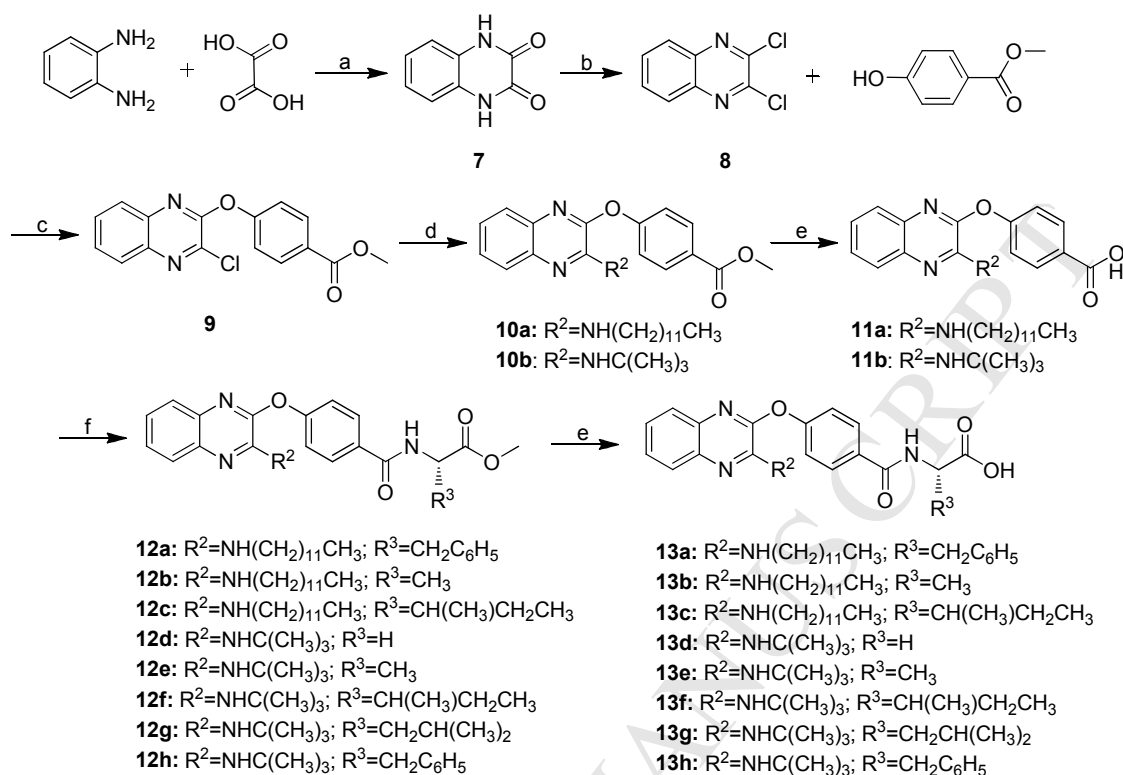
To obtain series I compounds **5a-e** & **6a-g** (R²=methyl), the general synthetic steps outlined in Scheme 1 were adopted. Briefly, the condensation of commercially available *o*-phenylenediamine with ethyl pyruvate led to the formation of quinoxalinone core **1**. It should be noted that when 4-chloro *o*-phenylenediamine was used as starting material, the reaction with ethyl pyruvate gave a mixture of two positional isomers, 6-chloro-3-methylquinoxalin-2(1*H*)-one (**1b**) and 7-chloro-3-methylquinoxalin-2(1*H*)-one (**1c**), under the same reaction condition. The isomer **1b**, which has slightly lower polarity (higher *R_f* value on the TLC plate), can also be regioselectively prepared according to our previously reported method [40]. After separation through flash column chromatography, the chemical structures of these two isolated isomers (**1b** and **1c**), can be easily distinguished based on respective ¹H NMR spectrum information (see Experimental section). Subsequent chlorination followed by nucleophilic substitution by using methyl 4-hydroxybenzoate in the presence of K₂CO₃ gave the *O*-substituted ester compound **3** with relatively high yield (>80%). After purification with conventional column chromatography method, the ester intermediate **3** was then subjected to hydrolysis under alkaline condition to generate the corresponding carboxylic acids **4a-c**. This was followed by coupling with various L-amino acid methyl ester hydrochlorides in the existence of isobutyl chloroformate and *N*-methylmorpholine (NMM) in anhydrous THF to yield the quinoxaline peptidomimetic esters **5a-e**. In this reaction, apart from THF, other aprotic polar solvents, *e.g.* dichloromethane (CH₂Cl₂) and

N,N-dimethylformamide (DMF), are possible alternatives. The quinoxaline peptidomimetic esters (**5a-g**) were further subjected to hydrolysis process to afford the final products **6a-g**.



Scheme 1. Synthetic procedures of quinoxaline peptidomimetic derivatives **5a-e** and **6a-g**. Reagents and conditions: (a) Ethyl pyruvate, anhydrous EtOH, rt; (b) POCl₃, reflux; (c) K₂CO₃, DMF, 85°C; (d) LiOH, Dioxane/H₂O (3:1, v:v); (e) L-amino acid methyl ester hydrochloride, isobutyl chloroformate, 4-Methylmorpholine, anhydrous THF, 0°C to r.t.

The synthetic protocol of quinoxaline peptidomimetic derivatives **12a-b** & **13a-h** ($R^2 = \textit{tert}$ -butylamine or dodecylamine moieties) is illustrated in Scheme 2. The condensation of unsubstituted *o*-phenylenediamine with oxalic acid led to quinoxaline-2,3(1*H*,4*H*)-dione **7**. After treating compound **7** with POCl₃ under refluxing condition, the chlorinated intermediate **8** was obtained, which was subjected to the subsequent nucleophilic substitution with methyl 4-hydroxybenzoate and alicyclic amines in the presence of weak bases, K₂CO₃ and triethylamine (TEA), respectively, and was converted to the key ester intermediates **10a** and **10b**. These esters were then treated by ester hydrolyzation, condensation, and another round of ester hydrolyzation to afford the products **13a-h**.



Scheme 2. Synthetic procedures of quinoxaline peptidomimetic derivatives **12a-h** and **13a-h**. Reagents and conditions: (a) Conc. HCl, reflux; (b) POCl₃, reflux; (c) K₂CO₃, DMF, 85°C; (d) R²NH₂, TEA, DMSO, 75°C; (e) LiOH, Dioxane/H₂O (3:1, v:v); (f) L-amino acid methyl ester hydrochloride, isobutyl chloroformate, 4-Methylmorpholine, anhydrous THF, 0°C to r.t.

2.2. Anti-proliferative evaluation and structure-activity relationships (SARs) examination

Under the guidance of activity evaluation of topo II inhibitors [41], compounds **5a-e**, **6a-g**, **12a-b** and **13a-h** were initially screened for their anti-proliferative and cytotoxic efficacies against a panel of topo II inhibitor-sensitive human tumor cell lines by MTT assay (Table 1). Topo II inhibitor Doxo was used as a positive control.

In general, the vast majority of test compounds displayed moderate anti-proliferative activities against tumor cell proliferation, except two ester compounds (**12d** and **12g**) and one carboxylic acid compound (**13d**) which did not exhibit obvious cytotoxicity. Besides, all carboxylic acid compounds ($R^4 = \text{H}$) showed improved anti-proliferative activities compared with their precursor esters ($R^4 = \text{CH}_3$, entries **5a-g** vs. **6a-g**, **12a-h** vs. **13a-h**). This result confirmed the essential role of the free acid unit of XK469 on maintaining antitumor potency. It is likely that this free acid motif can provide more effective hydrogen-bonding interactions with target protein, which may benefit the protein backbone-binding affinity. Generally, the carboxylic acid compounds may enable potential oral bioavailability in comparison with the less-active ester counterparts, largely due to better aqueous solubility.

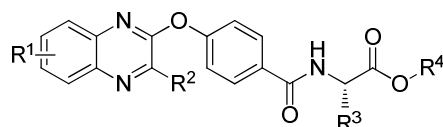
Among these compounds, when R² group is fixed as a methyl group, the impact of R¹ group on quinoxaline core was subsequently examined. It indicated that Cl atom (entries **5b**, **5e**, **5g**) did not contribute to a dramatically elevated antitumor efficacy compared with XK469, implying halogen element may not be a determining factor for the bioactivity of these compounds. However, changing halogen substitution from the C-6 position to the C-7 position (entries **5e** vs. **5g** and **6e** vs. **6g**) resulted in moderately improved activity, which is partially similar to the SAR of XK469. Following these clues, the R¹ group in compounds **12** and **13** was fixed as H atom, and then we turned our attention to the influence of *tert*-butylamine or dodecylamine moiety.

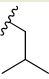
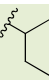

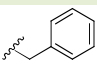
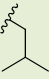
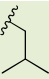
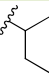
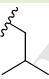
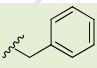

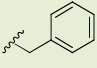
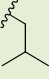
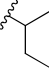
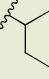
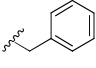
In all series, compounds **13a** and **13b** that possess *tert*-butylamine or dodecylamine fragment at the 3-position of quinoxaline core generated better anti-proliferative potencies than Doxo, while **13f** that possesses *tert*-butylamine and L-propionic acid showed cytotoxicity comparable with that of control. These results indicated the critical function of R² substitution. Thus, to a certain extent, it proved our design concept on XK467 analogues. However, compounds **12d**, **12g**, **13d** and **13g** with the same pharmacophore-like groups, showed significantly impaired potencies. This result might be largely attributed to the inappropriate size and/or orientation of aliphatic *sec*-butyl group of isoleucine, making these four compounds cannot accommodate the active binding area of target protein. Likewise, other compounds with *sec*-butyl group (entries **5c** and **6c**) also demonstrated reduced *in vitro* cytotoxicity.

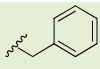
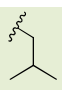
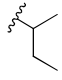
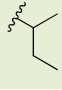
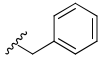
Finally, when fixing the R³ group as a methyl or benzyl group, the efficacies of **13a** and **13b** (R² = dodecylamine fragment) are superior to that of entries **13e** and **13h** (R² = *tert*-butylamine unit). A possible explanation was that the flexibility of long chain dodecyl group made it be more suitable for fitting the active binding pocket (pocket II) of the topo II. But it seemed that this finding cannot be applied to compounds **13d** and **13g**, whose R² substituent is a *sec*-butyl group. Although both compounds have weak or even no activity, **13g** with *tert*-butylamine portion resulted in a slightly increased activity compared with the dodecylamine substituted counterpart **13d**. This comparison suggests that the negative effect by attaching a *sec*-butyl group to the R³ position.

In brief, in regard to the inhibitory effects, although almost all tested compounds exerted similar cytotoxicity towards selected tumor cells in this study, most of them gave elevated anti-proliferative activities than the prototype XK469 reported previously. According to the NCI anti-proliferative assessment towards 60 tumor cells, the average IC₅₀ value of XK469 is about 70μM [8]. Although the quinoxaline peptidomimetic analogues tend to have similar action mechanism as that of XK469, they are likely to yield better anti-proliferative efficacies. Among these XK469 derivatives, two compounds with dodecylamine segment, **13a** and **13b** in particular, exhibited obviously improved cytotoxicity.

Table 1. Chemical structures and anti-proliferative activities of XK469 analogues.



Compds	R ¹	R ²	R ³	R ⁴	MCF-7 IC ₅₀ (μM) ^a	K562 IC ₅₀ (μM) ^a	Hela IC ₅₀ (μM) ^a
5a	H	CH ₃	CH ₃	CH ₃	38.43 ± 8.1	45.54 ± 20.9	32.20 ± 4.4 ^{**}
5b	H	CH ₃		CH ₃	25.53 ± 0.34	22.63 ± 0.36	21.55 ± 0.37
5c	H	CH ₃		CH ₃	36.14 ± 3.8	38.26 ± 13.6	>50
5d	6-Cl	CH ₃	CH ₃	CH ₃	33.77 ± 2.1 ^{**}	26.02 ± 3.8	42.51 ± 20.9
5e	6-Cl	CH ₃		CH ₃	22.75 ± 0.82	32.56 ± 0.32	37.55 ± 0.32
5f	7-Cl	CH ₃		CH ₃	25.52 ± 0.36	27.53 ± 0.32	28.76 ± 3.6 [*]
5g	7-Cl	CH ₃		CH ₃	19.05 ± 0.1	22.01 ± 2.0	18.64 ± 0.5 ^{**}
6a	H	CH ₃	CH ₃	H	25.55 ± 2.0	28.06 ± 2.6	22.31 ± 3.5
6b	H	CH ₃		H	14.72 ± 0.49 [*]	19.51 ± 0.16	17.32 ± 1.6
6c	H	CH ₃		H	35.71 ± 1.5	30.50 ± 1.2	33.24 ± 2.1
6d	6-Cl	CH ₃	CH ₃	H	19.45 ± 3.7	20.85 ± 6.8 [*]	29.99 ± 8.0
6e	6-Cl	CH ₃		H	17.41 ± 4.8 ^{**}	21.33 ± 1.3	25.02 ± 1.1
6f	7-Cl	CH ₃		H	20.15 ± 3.2	21.51 ± 1.2 [*]	20.21 ± 5.1
6g	7-Cl	CH ₃		H	15.11±6.6	14.52±2.8	16.35 ± 0.4
12a	H	NH(CH ₂) ₁₁ CH ₃		CH ₃	33.43 ± 3.8	30.50 ± 0.1	34.44±4.7 ^{**}
12b	H	NH(CH ₂) ₁₁ CH ₃	CH ₃	CH ₃	33.77 ± 2.1 ^{**}	26.72 ± 8.3 [*]	28.48 ± 0.48
12c	H	NH(CH ₂) ₁₁ CH ₃		CH ₃	43.26 ± 3.8 ^{**}	30.77 ± 9.1	40.3 ± 1.3 ^{**}
12d	H	NH(CH ₂) ₁₁ CH ₃		CH ₃	>50	>50	>50
12e	H	NH(CH ₂) ₁₁ CH ₃	H	CH ₃	38.43 ± 2.1 ^{**}	42.23 ± 20.1	55.16 ± 8.5
12f	H	NHC(CH ₃) ₃	CH ₃	CH ₃	33.44 ± 4.6 ^{**}	38.7 ± 5.3	31.9 ± 1.9 [*]
12g	H	NHC(CH ₃) ₃		CH ₃	>50	>50	>50
12h	H	NHC(CH ₃) ₃		CH ₃	>50	10.31 ± 1.7 [*]	>50

13a	H	NH(CH ₂) ₁₁ CH ₃		H	6.79 ± 0.17	7.37 ± 0.14	9.19 ± 0.42
13b	H	NH(CH ₂) ₁₁ CH ₃	CH ₃	H	4.11 ± 0.24	3.28 ± 0.28**	6.24 ± 0.27
13c	H	NH(CH ₂) ₁₁ CH ₃		H	30.42 ± 0.68	21.54 ± 0.31	35.46 ± 3.7*
13d	H	NH(CH ₂) ₁₁ CH ₃		H	>50	>50	>50
13e	H	NH(CH ₂) ₁₁ CH ₃	H	H	29.44 ± 5.8**	26.41 ± 11.14	23.43 ± 5.33*
13f	H	NHC(CH ₃) ₃	CH ₃	H	11.35 ± 0.37	18.34 ± 0.58*	13.36 ± 0.23
13g	H	NHC(CH ₃) ₃		H	40.32 ± 0.43	42.33 ± 0.46	39.19 ± 3.8**
13h	H	NHC(CH ₃) ₃		H	25.34 ± 0.38	15.22 ± 1.5*	20.50 ± 13.63
Doxo					8.81 ± 0.11	13.53 ± 1.3	11.50 ± 0.45

^a Values are means of three experiments, standard deviation is given. * $p < 0.01$, ** $p < 0.05$ compared to the control (Doxo).

2.3. Anti-metastatic activity in vivo

In vivo anti-metastatic evaluation was subsequently conducted. Human H22 hepatocarcinoma cells metastatic cancer BALB/c mouse model was utilized following the protocol described by our previous works [42, 43]. Five compounds revealing obvious anti-proliferative activities at cellular levels (**6b**, **6g**, **13a**, **13b**, **13f**) were subjected to the *in vivo* assessment through intragastric administration. The anti-metastatic ability of these compounds was measured based on the inhibition of H22 cell localization in the lungs.

As shown in Table 2, it demonstrated that the *in vivo* anti-tumor results using this model are in accordance with that of *in vitro* anti-proliferative investigation. Moreover, an obvious weight loss was not observed during continuous administration, suggesting mice could be continually experienced the maximum tolerance dosage. However, all tested compounds exhibited lower inhibitory rates compared with the control (Doxo, 59.89%), with the values of 33.71% (entry **13a**), 42.47% (entry **13b**), 27.60% (entry **13f**), 14.77% (entry **6g**) and 10.98% (entry **6b**), respectively. This result might be attributed to the first-pass effect by using intragastric administration, leading to ineffective absorption metabolized through gastrointestinal tract. In this circumstance, developing more effective antitumor agents *via* structural optimization or attempting other routes of administration (*e.g.* intravenous or intraperitoneal injection) is expected to increase the metabolic stability and achieve improved bioavailability.

Another fascinating aspect that is connected to this *in vivo* evaluation is that relatively high levels of XK469 (approximate 74.4 mg/kg) is tolerated to exert the therapeutic effects on tumor-bearing mice reported previously [8], while the dosages used in this assay (10 mg/kg) is much lower than that of XK469.

This result alluded that these newly identified quinoxaline peptidomimetic derivatives, **13a** and **13b** in particular, which exhibited promising *in vitro* cytotoxicity and *in vivo* anti-metastatic activities, might generate more potent curative efficacies than XK469. However, owing to the lower activity than the control Doxo, further deliberate chemical optimization is still needed to generate more effective tool compounds for tumor therapeutic screening.

Table 2. *In vivo* anti-metastatic effects of selected compounds.

Compds	Survived mice (n)	Body weight (g)	Lung weight (g)	Metastasized nodes on lung surface (n)	Inhibitory rate (%)
6b	10	22.46 ± 3.22	0.238 ± 0.024	18.23 ± 9.44**	10.98
6g	10	23.25 ± 4.14	0.254 ± 0.033*	17.14 ± 6.11**	14.77
13a	9(10)	20.85 ± 3.79	0.197 ± 0.025	13.33 ± 4.14**	33.71
13b	9(10)	24.62 ± 3.82	0.230 ± 0.040*	11.67 ± 6.73	42.47
13f	10	21.84 ± 5.58	0.211 ± 0.027	14.56 ± 7.54*	27.60
Doxo	9(10)	23.32 ± 1.80	0.217 ± 0.021	8.11 ± 3.33	59.89
Blank	10	20.17 ± 3.66	0.287 ± 0.117	20.11 ± 7.84	–

^a The animal number in parentheses is the original number; ^b Blank control means 0.5% CMC-Na; **P*<0.05; ***P*<0.01.

2.4. Topo II-mediated kinetoplast DNA (kDNA) decatenation assay

Given evidences have revealed that XK469 might selectively inhibit DNA topo II, rather than topo I, the topo II-mediated kDNA decatenation assay was thereby implemented to validate the possible mechanism of action of selected compounds, according to the formation of decatenated kDNA. Based on the biochemical activity of topo II, inhibition of topo II activity leads to the accumulation of catenated kDNA [44]. In this assay, two potent compounds (**13a** and **13b**) that stood out from the *in vitro* and *in vivo* screening were utilized. The validated topo II inhibitor, etoposide, was utilized as a positive control. The results evinced that both inhibited the formation of decatenated kDNA examined by agarose gel electrophoresis, as shown in Fig. 4. Especially, compound **13a** gave the best kDNA decantation inhibition and was approximate 4 times more active than the control. Another compound **13b** showed comparable potencies with the control. Dose-dependent aggregations of kDNA induced by two compounds were clearly observed at four tested concentrations of 3.15, 12.5, 50 and 200 µM, higher than or comparable with that of etoposide at the same concentrations. In short, these preliminary results indicated that these quinoxaline peptidomimetic analogues of XK469 might work as topo II inhibitors, similar to the prototype XK469.

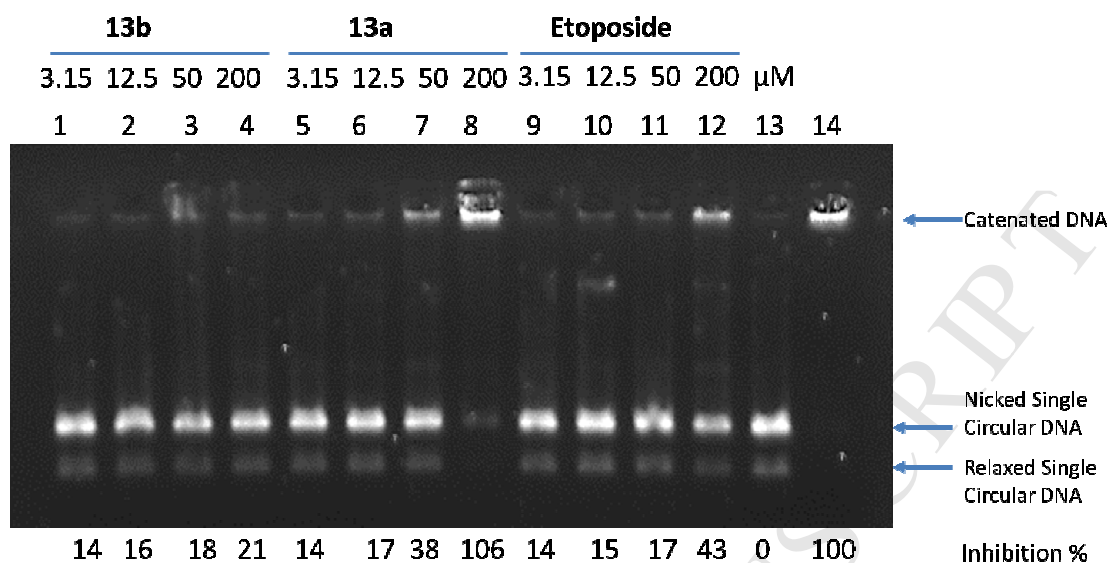


Fig. 4. Selected compounds (**13a** and **13b**) inhibited topo II-mediated kinetoplast DNA (*k*DNA) decatenation to form minicircular DNA. Lane 14: Negative control without topo II; Lane 13: Positive control that contains topo II but without inhibitors; Lanes 9–12: Topo II inhibitor etoposide (control) at four tested concentrations of 3.15, 12.5, 50 and 200 μ M; Lanes 1–8: Tested compounds at the same concentrations.

2.5. Molecular docking study

Compound **13b** was derived from XK469 and they showed comparable potencies, which was thereby utilized as a model in molecular docking exploration. Structural configurations of prototype XK469 and **13b** were initially optimized *via* ChemBio3D Ultra program, and their superimposed conformations were compared *via* overlapping operation using Sybyl program. Figures 5(a) and 5(b) displayed their preferential conformations. Fig. 5(c) exhibited that the skeletal backbones of two compounds adopted very similar spatial orientation, suggesting identical affinity to the same spatial regions (pocket I, II and III).

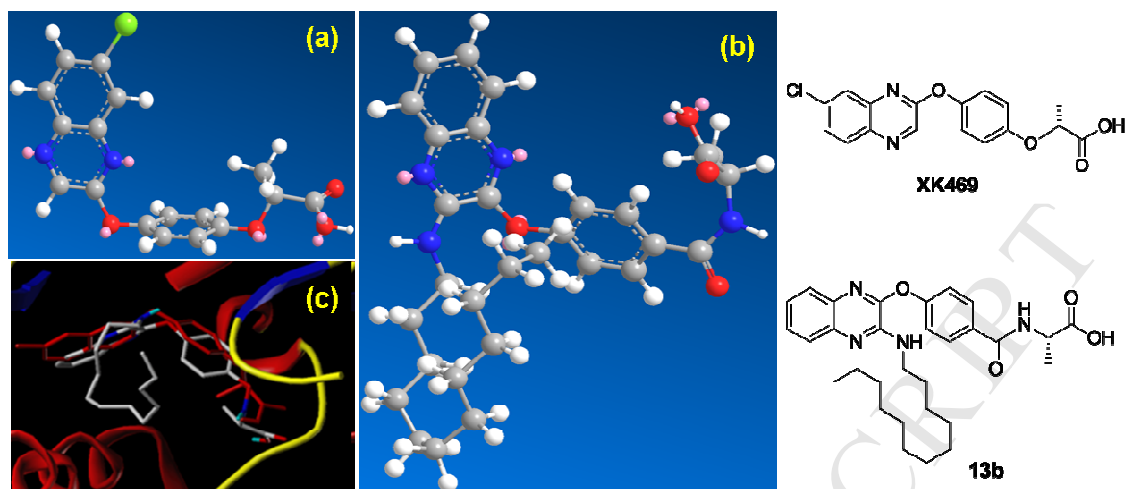


Fig. 5. The comparison of optimized configurations of XK469 (a) and 13b (b) *via* ChemBio3D Ultra program, and superimposed conformations of XK469 (red) and 13b (gray) (c) signified similar three-dimensional topology and binding affinity.

The interactions between **13b** and topo II (PDB ID: 1ZXN) were further examined by molecular docking program. As displayed in Fig. 6, **13b** could commendably bind to the ATPase domain of topo II. Both quinoxaline core and terminal carboxylic acid motif of **13b** could fit well into the hydrophobic pocket I and III of topo II, leading to possible enzymatic inhibition, consistent with their bioactivity results. Moreover, the bulk and flexible long chain dodecyl group could undergo low-energy conformational change to accommodate the long hydrophobic cavity of topo II (pocket II). In addition to these effective hydrophobic interactions, several hydrogen-bonding contacts between **13b** and key amino acids in the ATPase domain of topo II also contribute to the enhanced protein backbone-binding affinity. Specifically, the 1-N of **13b** acts as an H-bonding acceptor to interact with the peripheral NH of the Asn91, with a distance of 2.20Å. Besides, amide O of the peptidomimetic functional group of **13b** also serves as an H-bonding acceptor to bind with Ser149 residue (2.43Å). Finally, both carbonyl O and terminal hydroxyl O of **13b** work as H-bonding acceptors to interact with Asn91 (2.16Å), Ala167 (2.58Å and 1.83Å), and Lys168 (2.74Å), respectively.

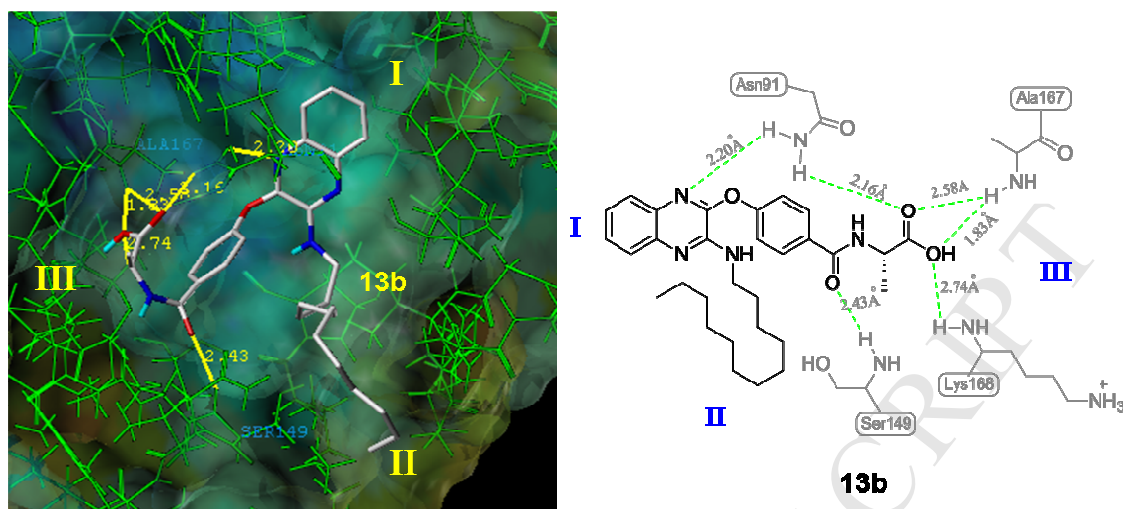


Fig. 6. Binding pattern of compound **13b** with the active binding pockets of topo II (PDB code: 1ZXN).

Comparing the binding modes of **13b** and XK469, **13b** not only provided more effective H-bonding contacts, but also generated more hydrophobic interactions through well occupation of three hydrophobic pockets (I, II and II) of topo II. As a result, **13b** might be more potent than the prototype XK469 in achieving potential anti-tumor drugs. Further biological assessments of **13a** and **13b** are underway and the updated results will be reported in the near future.

3. Conclusion

In the present work, we report the design, synthesis, biological evaluation, biochemical assay, and binding mode of novel quinoxaline peptidomimetic derivatives as potent antitumor agents. These compounds exhibited obvious cytotoxicity against three tumor cell lines (MCF-7, K562 and Hela). Subsequent *in vivo* anti-metastatic evaluation also supported the antitumor effects of these compounds, especially compounds **13a** and **13b**. SAR exploration implicated that *tert*-butyl or dodecyl moiety at the 3-position of quinoxaline core was favorable to fit the ATPase pocket of topo II and contribute to improved antineoplastic activities. The dodecyl moiety is proved to be more favored than that of *tert*-butylamine motif, although both of these two motifs could lead to somehow improved anti-proliferative potencies against selected cell lines. Moreover, the free carboxylic acid unit of XK469 is important to maintain the antitumor activity. Additionally, topo II-mediated *k*DNA decatenation assay also preliminarily confirmed that these derivatives are potent topo II inhibitors.

Lastly, molecular modeling of prototype XK469 and **13b** offers a visual framework for understanding the structural basis for their topo II inhibitory activities, and might reveal a general strategy for design and screen more potent topo II inhibitors. In specific, **13b**, a peptidomimetic analogue of XK469 with a flexible long chain dodecyl group, adopted a very similar 3D topology and spatial orientation compared with XK469. It implies that compounds reported in this paper might share similar mechanism of action with the prototype XK469. The detailed mechanism of action of these derivatives is under investigation.

Based on the biochemical and biological results, we envisioned that quinoxaline peptidomimetic derivatives **13a** and **13b** might be promising candidates for further chemical optimization. In particular, the introduced R² hydrophobic dodecyl unit of these two compounds may not only be critical for elevated antitumor activities through enhancing protein backbone binding interactions, but also contribute to improved pharmacokinetic properties *via* albumin binding. Overall, we anticipated these identified quinoxaline peptidomimetic derivatives may provide a clue for researchers to develop more diversified compounds with improved antineoplastic activities.

4. Experimental section

4.1. Chemistry

4.1.1. General

All the starting materials including reagents and solvents, unless otherwise specified, were analytically pure and obtained from commercial suppliers. They were used without further purification, when necessary, were purified and dried by standard protocols. All reactions except those in aqueous media were carried out by standard techniques for the exclusion of moisture. All reaction progress was monitored by thin-layer chromatography (TLC) on 0.25-mm silica gel plates (grade 60, GF₂₅₄) and visualized with UV light (254nm), or iodine vapor. Flash chromatography was performed on silica gel (Yantai Muping Inc., 300–400 mesh). Melting points were determined using X-6 digital display binocular microscope (uncorrected). ¹H NMR and ¹³C NMR spectra were recorded on a Bruker Advance 300 or DRX-400 spectrometer using CDCl₃ or DMSO-*d*₆ as solvents, TMS as an internal standard. Chemical shift values (δ) are reported in parts per million (ppm) and the coupling constants (*J*) are given in hertz (Hz), and splitting patterns are designated as follows: s, single; d, doublet; t, triplet; q, quartet; m, multiplet. Electrospray ionization mass spectrometry (ESI–MS) data were collected on a Micromass Qtof-Micro LC–MS instrument.

4.1.2. General synthetic procedure for the preparation of 3-methylquinoxalin-2(1*H*)-one (**1**)

o-Phenylenediamine (92.6 mmol, 10 g) was suspended in anhydrous ethanol (100 mL). The mixture was then cooled in an ice bath. A solution of ethyl pyruvate (202.9 mmol, 23.54g) in anhydrous ethanol (20 mL) was added dropwise over a period of 20 min under stirring. The resulting solution was allowed to react at room temperature for 6 h until the TLC showed the reaction has completed. The resulting precipitate was filtered and washed with anhydrous ethanol (2 × 15 mL), and dried in vacuum to give the desire product **1a** (14.1 g, 95%) as white solid which was pure enough for further reaction. M.p: 241.0–242.7 °C; ESI-MS *m/z*: 161.0 [M+H]⁺.

Using 4-chlorobenzene-1,2-diamine as starting material, the reaction with ethyl pyruvate under the same condition with **1a** gave two positional isomers, 6-chloro-3-methylquinoxalin-2(1*H*)-one (**1b**) and 7-chloro-3-methylquinoxalin-2(1*H*)-one (**1c**).

4.1.2.1.6-Chloro-3-methylquinoxalin-2(1*H*)-one (**1b**). Light yellow powder, yield: 54%, mp: 263.0–264.0

°C. ¹H NMR (400 MHz, DMSO-*d*₆) δ: 12.36 (s, 1H, NH), 7.68~7.70 (d, *J* = 8.4 Hz, 1H, ArH), 7.27~7.30 (dd, *J*₁ = 8.4 Hz, *J*₂ = 2.3 Hz, 1H, ArH), 7.26 (d, *J* = 2.3 Hz, 1H, ArH), 2.39 (s, 3H, CH₃); ESI-MS *m/z*: 195.3 [M+H]⁺.

4.1.2.2. 7-Chloro-3-methylquinoxalin-2(1H)-one (**1c**). Light yellow powder, yield: 43%, mp: 265.0~267.0 °C. ¹H NMR (400 MHz, DMSO-*d*₆, ppm) δ: 12.41 (s, 1H, NH), 7.74~7.75 (d, *J* = 2.3 Hz, 1H ArH), 7.51~7.53 (dd, *J*₁ = 8.7 Hz, *J*₂ = 2.3 Hz, 1H, ArH), 7.27~7.29 (d, *J* = 8.7 Hz, 1H, ArH), 2.41 (s, 3H, CH₃); ESI-MS *m/z*: 195.3 [M+H]⁺.

4.1.3. General procedure for 2-chloro-3-methyl substituted quinoxaline (**2**)

Compound **1a** (28.1 mmol, 5.0 g) was dissolved in POCl₃ (25 mL) at 0°C, the resulting solution was allowed to reflux at 120°C for 5 h. After completion of reaction, the reaction was quenched with cooled ammonia, which was further extracted with ethyl acetate (EtOAc, 2 × 15 mL). The organic phase was separated and washed with brine, dried over anhydrous MgSO₄, filtered, and concentrated in *vacuum* to afford the crude product, which was purified by silica gel flash chromatography (PE : EA = 10:1, v:v) to afford 5.0 g of **2a** as a off-white solid, yield 90%. M.p.: 86.0~87.0 °C; ESI-MS *m/z*: 179.4 [M+H]⁺.

4.1.3.1. 2,6-Dichloro-3-methylquinoxaline (**2b**). White powder, yield: 89%, ESI-MS *m/z*: 213.8 [M+H]⁺; mp: 128.2~129.3 °C.

4.1.3.2. 3,6-Dichloro-2-methylquinoxaline (**2c**). White powder, yield: 86%, ESI-MS *m/z*: 214.1 [M+H]⁺; mp: 132.1~133.2 °C.

4.1.4. General procedure for methyl 4-((substituted 3-methylquinoxalin-2-yl)oxy)benzoate (**3**)

Methyl 4-hydroxybenzoate (42.1 mmol, 6.4 g) and K₂CO₃ (50.5 mmol, 5.3 g) were dissolved in DMF (150 mL), the resulting solution was allowed to react at 85°C for 12 h. Compound **2a** (23.5 mmol, 5.0 g) was added in batches, and the resulting mixture was allowed to react for additional 12h at the same condition. After completion of reaction, the reaction was quenched with cooled water (150 mL) and extracted with EtOAc (2 × 100 mL). The combined organic phase was washed with brine, dried over anhydrous MgSO₄, filtered, and concentrated in *vacuum* to afford the crude product, which was purified by silica gel flash chromatography (PE : EA = 50:1, v:v) to afford 6.6 g of **3a** as oily semi- solid, yield 80%. ESI-MS *m/z*: 295.4 [M+H]⁺.

4.1.4.1. Methyl 4-((6-chloro-3-methylquinoxalin-2-yl)oxy)benzoate (**3b**). Oily semi-solid, yield 68%; ESI-MS *m/z*: 329.8 [M+H]⁺.

4.1.4.2. Methyl 4-((7-chloro-3-methylquinoxalin-2-yl)oxy)benzoate (**3c**). Oily semi-solid, yield 59%; ESI-MS *m/z*: 329.6 [M+H]⁺.

4.1.5. General procedure for 4-((substituted 3-methylquinoxalin-2-yl)oxy)benzoic acid (**4**)

Methyl 4-((3-methylquinoxalin-2-yl)oxy)benzoate (8.0 mmol, 2.0 g) and LiOH (24.0 mmol, 0.85 g) were suspended in a mixture of dioxane (15 mL) and water (5 mL) at 0°C, the resulting suspension was reacted for 5h. After the removal of solvent, 20 mL of distilled water was added and the mixture was

washed with EtOAc (2×10 mL). Then the combined water phase was acidified with 2N HCl and the precipitate was collected, which was recrystallized with MeOH/H₂O (3:1, v:v) to afford 1.8 g of the pure product 4-((3-methylquinoxalin-2-yl)oxy)benzoic acid (**4a**) as white semi-solid. Yield 95%; ¹H NMR (400 MHz, DMSO-*d*₆) δ : 13.03 (s, 1H, COOH), 8.06–8.08 (d, J = 8.4 Hz, 2H, ArH), 7.99 (s, 1H, ArH), 7.66 (s, 3H, ArH), 7.45–7.47 (d, J = 8.4 Hz, 2H, ArH), 2.76 (s, 3H, CH₃) ppm; ¹³C NMR (100 MHz, DMSO-*d*₆) δ : 166.66, 148.04, 139.02, 138.52, 131.09, 129.44, 127.80, 127.66, 126.81, 121.82, 20.28 ppm; ESI-MS m/z : 281.3 [M+H]⁺.

4.1.5.1. 4-((6-Chloro-3-methylquinoxalin-2-yl)oxy)benzoic acid (**4b**). Semi-solid, yield 90%; ¹H NMR (400 MHz, DMSO-*d*₆) δ : 13.04 (s, 1H, COOH), 8.06–8.08 (d, J = 8.0 Hz, 3H, ArH), 7.68 (s, 2H, ArH), 7.40–7.48 (m, 2H, ArH), 2.76 (s, 3H, CH₃) ppm; ¹³C NMR (100 MHz, DMSO-*d*₆) δ : 167.13, 156.64, 149.65, 139.64, 137.30, 131.60, 130.29, 129.06, 126.69, 122.36, 100.03, 20.85 ppm; ESI-MS m/z : 315.5 [M+H]⁺.

4.1.5.2. 4-((7-Chloro-3-methylquinoxalin-2-yl)oxy)benzoic acid (**4c**). Semi-solid, yield 91%; ¹H NMR (400 MHz, DMSO-*d*₆) δ : 12.99 (s, 1H, COOH), 8.05–8.07 (d, 2H, J = 8.0 Hz, ArH), 7.99–8.01 (m, 1H, ArH), 7.67–7.73 (m, 2H, ArH), 7.45–7.47 (d, J = 8.0 Hz, 2H, ArH), 2.74 (s, 3H, CH₃) ppm; ¹³C NMR (100 MHz, DMSO-*d*₆) δ : 167.18, 156.57, 156.26, 150.01, 140.10, 138.01, 132.86, 131.61, 130.30, 129.17, 128.47, 122.40, 120.44, 20.88 ppm; ESI-MS m/z : 315.7 [M+H]⁺.

4.1.6. General procedure for the synthesis of ester compound (**5**)

To a solution of ester compound **4a** (1.8 mmol, 0.5 g) in anhydrous THF (15 mL) at -5°C was added isobutyl chloroformate (2.2 mmol, 300 mg) and *N*-methylmorpholine (NMM, 2.2 mmol, 220 mg) successively. After stirred at the same temperature for 30min, L-alanine methyl ester hydrochloride (2.0 mmol, 142 mg) was added in small portions. Then the mixture was stirred at room temperature for 4h until the completion monitored by TLC, which was then concentrated and extracted with EtOAc (2×50 mL). Layers were separated and the organic layer was washed in turn with 1N HCl (20 mL), saturated NaHCO₃ (20mL) and brine (2×15 mL), dried over anhydrous Na₂SO₄, filtered, and evaporated in *vacuo*, and the obtained crude compound was purified by flash chromatography (PE : EA = 5:1 to 4:1, v:v) to afford 370 mg of **5a** as white solid, yield 58%. M.p. 161–162°C; ¹H NMR (400 MHz, CDCl₃) δ : 7.97–8.00 (dd, J_1 = 6.0 Hz, J_2 = 3.7 Hz, 1H ArH), 7.91–7.94 (d, J = 8.7 Hz, 2H, ArH), 7.67–7.70 (m, 1H, ArH), 7.58–7.61 (m, 2H, ArH), 7.35–7.36 (d, J = 8.7 Hz, 2H, ArH), 6.77–6.79 (d, J = 7.0 Hz, 1H, ArH), 4.80–4.88 (dd, J_1 = 14.3, J_2 = 7.2 Hz, 1H, CH), 3.82 (s, 3H, OCH₃), 2.83 (s, 3H, CH₃), 1.55–1.57 (d, J = 7.1 Hz, 3H, CH₃). ¹³C NMR (100 MHz, CDCl₃) δ : 173.74, 166.11, 155.75, 155.55, 147.85, 139.61, 139.22, 130.85, 129.29, 128.71, 128.07, 127.60, 127.31, 121.81, 52.65, 48.57, 20.62, 18.73 ppm; ESI-MS m/z : 366.5 [M+H]⁺.

The following compounds **5b–5g** were prepared according to the general procedures as described for the preparation of compound **5a**.

4.1.6.1. (*S*)-Methyl 4-methyl-2-(4-((3-methylquinoxalin-2-yl)oxy)benzamido)pentanoate (**5b**). White solid, yield: 52%; m.p. = 166–169°C; ¹H NMR (400 MHz, DMSO-*d*₆) δ: 7.97–8.00 (dd, *J*₁ = 8.0 Hz *J*₂ = 4.0 Hz, 1H, ArH), 7.91–7.93 (d, *J* = 8.0 Hz, 2H, ArH), 7.68–7.69 (d, *J* = 4.0 Hz, 1H, ArH), 7.58–7.61 (dd, *J*₁ = 8.0 Hz, *J*₂ = 4.0 Hz, 2H, ArH), 7.35–7.37 (d, *J* = 8.0 Hz, 2H, ArH), 6.53–6.55 (d, *J* = 8.0 Hz, 1H, NH), 4.87–4.90 (m, 1H, CH-C=O), 3.79 (s, 3H, OCH₃), 2.83 (s, 3H, CH₃), 1.71–1.77 (t, *J* = 8.0 Hz, 2H, CH₃), 1.67–1.69 (m, 1H, CH), 0.99–1.03 (m, 6H, 2×CH₃) ppm; ¹³C NMR (100 MHz, DMSO-*d*₆) δ: 173.85, 166.59, 156.00, 155.66, 148.02, 139.88, 139.40, 131.08, 129.42, 128.85, 128.25, 127.73, 127.48, 121.95, 52.56, 51.39, 42.19, 25.21, 23.00, 22.30, 21.17 ppm; ESI-MS *m/z*: 408.5 [M+H]⁺.

4.1.6.2. (2*S*,3*R*)-Methyl 3-methyl-2-(4-((3-methylquinoxalin-2-yl)oxy)benzamido)pentanoate (**5c**). White solid, yield: 55%; m.p. = 172–173°C; ¹H NMR (400 MHz, DMSO-*d*₆) δ: 7.98–8.00 (m, 1H, ArH), 7.91–7.93 (d, *J* = 8.0 Hz, 2H, ArH), 7.69–7.71 (m, 1H, ArH), 7.58–7.61 (m, 2H, ArH), 7.36–7.38 (d, *J* = 8.0 Hz, 2H, ArH), 6.67–6.69 (d, *J* = 8.0 Hz, 1H, NH), 4.84–4.87 (m, 1H, CH-C=O), 3.80 (s, 3H, OCH₃), 2.83 (s, 3H, CH₃), 1.26–1.31 (m, 1H), 0.97–1.01 (m, 2H, CH₂CH₃), 0.91–0.93 (d, *J* = 8.0 Hz, 6H, 2×CH₃), ppm; ¹³C NMR (100 MHz, DMSO-*d*₆) δ: 174.2, 170.8, 167.7, 158.8, 138.0, 137.7, 130.9, 129.4, 128.7, 128.2, 127.4, 127.1, 121.4, 57.6, 51.8, 38.2, 25.5, 17.1, 15.3, 12.1 ppm; ESI-MS *m/z*: 408.6 [M+H]⁺.

4.1.6.3. (*S*)-Methyl 2-(4-((6-chloro-3-methylquinoxalin-2-yl)oxy)benzamido)propanoate (**5d**). White solid, yield: 51%; m.p. = 180–181°C; ¹H NMR (400 MHz, DMSO-*d*₆) δ: 7.92–7.96 (m, 3H, ArH), 7.61–7.63 (d, *J* = 8.0 Hz, 1H, ArH), 7.53–7.55 (d, *J* = 8.0 Hz, 1H, ArH), 7.34–7.37 (m, 2H, ArH), 6.66 (d, *J* = 7.2 Hz, 1H, NH), 4.28–4.30 (d, *J* = 8.0 Hz, 1H, CH-C=O), 3.82 (s, 3H, OCH₃), 2.82 (s, 3H, CH₃), 1.57 (d, *J* = 7.2 Hz, 3H, CHCH₃) ppm; ¹³C NMR (100 MHz, DMSO-*d*₆) δ: 173.72, 166.02, 156.15, 155.39, 148.10, 139.74, 138.03, 134.99, 131.16, 129.20, 128.74, 128.38, 126.39, 121.90, 52.66, 48.58, 20.58, 18.72 ppm; ESI-MS *m/z*: 400.3 [M+H]⁺.

4.1.6.4. (*S*)-Methyl 2-(4-((6-chloro-3-methylquinoxalin-2-yl)oxy)benzamido)-4-methylpentanoate (**5e**). White solid, yield: 45%; m.p. = 156–158°C; ¹H NMR (400 MHz, CDCl₃) δ: 7.93–7.89 (t, *J* = 8.0 Hz, 3H, ArH), 7.69 (s, 1H, ArH), 7.52–7.54 (d, *J* = 8.0 Hz, 1H, ArH), 7.33–7.35 (d, *J* = 8.0 Hz, 2H, ArH), 6.54–6.56 (d, *J* = 8.0 Hz, 1H, NH), 4.87–4.90 (m, 1H, CH), 3.79 (s, 3H, OCH₃), 2.82 (s, 3H, CH₃), 1.58–1.59 (m, 1H, CH), 1.24–1.31 (m, 2H, CH₂), 0.99–1.03 (m, 6H, 2×CH₃) ppm; ¹³C NMR (100 MHz, CDCl₃) δ: 173.65, 166.40, 153.31, 155.41, 148.07, 139.60, 138.06, 134.99, 130.2, 129.20, 128.71, 128.36, 126.39, 121.87, 52.40, 51.24, 42.02, 25.05, 22.84, 22.13, 20.53 ppm; ESI-MS: *m/z*: 442.5 [M+H]⁺.

4.1.6.5. (*S*)-Methyl 2-(4-((7-chloro-3-methylquinoxalin-2-yl)oxy)benzamido)-3-phenylpropanoate (**5f**). White solid, yield: 40%; m.p. = 163–164°C; ¹H NMR (400 MHz, CDCl₃) δ: 7.87–7.88 (d, *J* = 2.0 Hz, 1H, ArH), 7.82 ~ 7.85 (dd, *J*₁ = 8.8 Hz, *J*₂ = 2.5 Hz, 3H, ArH), 7.65–7.68 (dd, *J*₁ = 8.8 Hz, *J*₂ = 2.0 Hz, 1H, ArH), 7.33–7.26 (m, 5H, ArH), 7.15–7.17 (d, *J* = 6.8 Hz, 2H, ArH), 6.60–6.62 (d, *J* = 7.4 Hz, 1H, NH), 5.10–5.15 (dd, *J*₁ = 13.0 Hz, *J*₂ = 5.6 Hz, 1H, CH-C=O), 3.79 (s, 3H, OCH₃), 3.27–3.32 (m, 2H, CH₂), 2.80 (s, 3H, CH₃) ppm; ¹³C NMR (100 MHz, CDCl₃) δ: 172.10, 166.14, 155.79, 155.50, 147.87, 139.61, 139.20,

135.84, 130.79, 129.37, 129.31, 128.69, 128.53, 128.07, 127.63, 127.32, 127.27, 121.78, 53.58, 52.50, 37.95, 20.62 ppm; ESI-MS: m/z : 476.4 $[M+H]^+$.

4.1.6.6. *(S)*-Methyl 2-(4-((7-chloro-3-methylquinoxalin-2-yl)oxy)benzamido)-4-methylpentanoate (**5g**).

White solid, yield: 40%; m.p. = 130–132°C; 1H NMR (400 MHz, DMSO- d_6) δ : 7.97–7.98 (d, J = 4.0 Hz, 1H, ArH), 7.91–7.93 (m, 2H, ArH), 7.60–7.63 (m, 1H, ArH), 7.53–7.55 (d, J = 8.0 Hz, 1H, ArH), 7.33–7.35 (d, J = 8.0 Hz, 2H, ArH), 6.54–6.56 (d, J = 8.0 Hz, 1H, NH), 4.89–4.90 (m, 1H, CH-C=O), 3.79 (s, 3H, OCH₃), 2.82 (s, 3H, CH₃), 1.33–1.34 (m, 1H, CH), 1.25–1.28 (m, 2H, CH₂), 0.99–1.03 (m, 6H, 2 \times CH₃) ppm; ^{13}C NMR (100 MHz, DMSO- d_6) δ : 173.68, 166.29, 155.95, 155.22, 149.20, 148.82, 139.87, 132.86, 131.43, 130.04, 128.71, 121.84, 52.42, 51.23, 42.01, 25.05, 22.84, 22.13, 20.61 ppm; ESI-MS: m/z : 442.5 $[M+H]^+$.

4.1.7. General procedure for the synthesis of carboxylic acid compound (**6**)

These compounds were synthesized according to similar procedures with that of compound (**4**).

4.1.7.1. *(S)*-2-(4-((3-Methylquinoxalin-2-yl)oxy)benzamido)propanoic acid (**6a**). White solid, yield: 66%; m.p. = 146–147°C; 1H NMR (400 MHz, DMSO- d_6) δ : 12.57 (s, 1H, COOH), 8.73–8.74 (d, J = 4.0 Hz, 1H, NH), 8.00–8.02 (t, J = 8.0 Hz, 3H, ArH), 7.65 (s, 3H, ArH), 7.42–7.45 (m, 2H, ArH), 4.42–4.46 (m, 1H, CH-C=O), 2.76 (s, 3H, CH₃), 1.41–1.42 (d, 3H, J = 4.0 Hz, CH₃) ppm; ^{13}C NMR (100 MHz, DMSO- d_6) δ : 174.72, 165.87, 156.20, 155.59, 148.51, 139.43, 139.09, 131.60, 129.92, 129.63, 128.29, 128.06, 128.17, 127.28, 122.16, 48.83, 20.82, 17.53 ppm; ESI-MS: m/z : 350.4 $[M-H]^-$.

4.1.7.2. *(S)*-4-Methyl-2-(4-((3-methylquinoxalin-2-yl)oxy)benzamido)pentanoic acid (**6b**). White solid, yield: 82%; m.p. = 143–144°C; 1H NMR (400 MHz, DMSO- d_6) δ : 12.61 (s, 1H, COOH), 8.67 (s, 1H, NH), 8.01–8.03 (d, J = 8.0 Hz, 3H, ArH), 7.65 (s, 3H, ArH), 7.43–7.45 (d, J = 8.0 Hz, 2H, ArH), 4.48 (s, 1H, CH-C=O), 2.77 (s, 3H, CH₃), 1.77–1.80 (d, J = 8.0 Hz, 2H, CH₂), 1.61 (m, 1H, CH), 0.91–0.94 (m, 6H, 2 \times CH₃) ppm; ^{13}C NMR (100 MHz, DMSO- d_6) δ : 174.77, 166.30, 156.22, 155.59, 148.48, 139.40, 139.08, 131.57, 129.91, 129.72, 128.28, 128.03, 127.26, 122.20, 51.40, 25.03, 23.49, 21.58, 20.83 ppm; ESI-MS: m/z : 392.3 $[M-H]^-$.

4.1.7.3. *(2S,3R)*-3-Methyl-2-(4-((3-methylquinoxalin-2-yl)oxy)benzamido)pentanoic acid (**6c**). White solid, yield: 85%; m.p. = 156–157°C; 1H NMR (400 MHz, DMSO- d_6) δ : 12.64 (s, 1H, COOH), 8.52–8.54 (d, J = 8.0 Hz, 1H, NH), 7.98–8.03 (m, 3H, ArH), 7.65–7.68 (m, 3H, ArH), 7.42–7.44 (d, J = 8.0 Hz, 2H, ArH), 4.34–4.38 (m, 1H, CH-C=O), 2.77 (s, 3H, CH₃), 1.04–1.08 (m, 1H, CH), 0.95–0.97 (d, J = 8.0 Hz, 3H, CH₃), 0.84–0.93 (m, 5H, CH₂CH₃) ppm; ^{13}C NMR (101 MHz, DMSO- d_6) δ : 173.73, 166.61, 156.24, 155.57, 148.51, 139.40, 139.08, 131.62, 129.90, 128.29, 128.04, 127.24, 122.12, 57.80, 36.16, 25.61, 20.84, 16.16, 11.54 ppm; ESI-MS: m/z : 392.7 $[M-H]^-$.

4.1.7.4. *(S)*-2-(4-((6-Chloro-3-methylquinoxalin-2-yl)oxy)benzamido)propanoic acid (**6d**). White solid, yield: 80%; m.p. = 133–135°C; 1H NMR (400 MHz, DMSO- d_6) δ : 12.4 (s, 1H, COOH), 8.72–8.73 (d, J = 7.1 Hz, 1H, NH), 8.02–8.04 (d, J = 8.6 Hz, 2H, ArH), 7.98–8.00 (d, J = 8.9 Hz, 1H, ArH), 7.66–7.72 (m,

2H, ArH), 7.44~7.45 (d, J = 8.4 Hz, 2H, ArH), 4.41~4.49 (m, 1H, CH-C=O), 2.75 (s, 3H, CH₃), 1.42~1.44 (d, J = 7.3 Hz, 3H, CH₃) ppm; ¹³C NMR (100 MHz, DMSO-*d*₆) δ : 174.72, 165.82, 156.80, 155.35, 149.23, 139.77, 138.01, 134.16, 131.70, 129.98, 129.67, 128.45, 126.15, 122.12, 48.79, 20.84, 17.47 ppm; ESI-MS: m/z : 386.6 [M-H]⁻.

4.1.7.5. (*S*)-2-(4-((6-Chloro-3-methylquinoxalin-2-yl)oxy)benzamido)-4-methylpentanoic acid (**6e**). White solid, yield: 80%; m.p. = 136~137°C; ¹H NMR (400 MHz, DMSO-*d*₆) δ : 12.54 (s, 1H, COOH), 8.65~8.67 (d, J = 8.0 Hz, 1H, NH), 7.99~8.04 (m, 3H, ArH), 7.74 (s, 1H, ArH), 7.67~7.69 (d, J = 8.0 Hz, 1H, ArH), 7.44~7.45 (d, J = 4.0 Hz, 2H, ArH), 4.47 (m, 1H, CH-C=O), 2.77 (s, 3H, CH₃), 1.77~1.83 (m, 2H, CH₂), 1.61~1.74 (m, 1H, CH), 0.90~0.95 (m, 6H, 2×CH₃) ppm; ¹³C NMR (100 MHz, DMSO-*d*₆) δ : 174.74, 166.27, 156.52, 155.40, 150.08, 139.70, 137.85, 132.04, 131.70, 130.25, 129.74, 129.01, 127.15, 122.21, 51.39, 25.02, 23.49, 21.58, 20.91 ppm; ESI-MS: m/z : 426.7 [M-H]⁻.

4.1.7.6. (2*S*,3*R*)-2-(4-((7-Chloro-3-methylquinoxalin-2-yl)oxy)benzamido)-3-methylpentanoic acid (**6f**). White solid, yield: 88%; m.p. = 148~149°C; ¹H NMR (400 MHz, DMSO-*d*₆) δ : 13.01 (s, 1H, COOH), 8.66~8.70 (m, 1H, NH), 7.98~8.01 (d, J = 8.0 Hz, 1H, ArH), 7.91~7.93 (d, J = 8.0 Hz, 2H, ArH), 7.75 (s, 1H, ArH), 7.66~7.69 (d, J = 8.0 Hz, 1H, ArH), 7.40~7.43 (m, 2H, ArH), 7.26~7.32 (m, 4H, ArH), 7.19~7.20 (d, J = 3.2 Hz, 1H, ArH), 4.57~4.63 (t, J = 12.0 Hz, 1H, CH-C=O), 3.02~3.25 (m, 2H, CH₂), 2.74 (s, 3H, CH₃) ppm; ¹³C NMR (100 MHz, DMSO-*d*₆) δ : 165.46, 156.67, 155.14, 149.40, 140.07, 139.45, 138.23, 132.32, 131.09, 130.08, 129.78, 129.38, 129.31, 128.41, 126.44, 122.67, 122.10, 55.71, 37.29, 20.88 ppm; ESI-MS: m/z : 426.4 [M-H]⁻.

4.1.7.7. (*S*)-2-(4-((7-Chloro-3-methylquinoxalin-2-yl)oxy)benzamido)-3-phenylpropanoic acid (**6g**). White solid, yield: 82%; m.p. = 176~177°C; ¹H NMR (400 MHz, DMSO-*d*₆) δ : 12.60 (s, 1H, COOH), 8.66~8.68 (d, J = 8.0 Hz, 1H, NH), 8.01~8.07 (m, 3H, ArH), 7.67 (s, 2H, ArH), 7.43~7.45 (d, J = 8.0 Hz, 2H, ArH), 4.44~4.50 (m, 1H, CH-CH=O), 2.77 (s, 3H, CH₃), 1.80~1.84 (t, J = 8.0 Hz, 2H, ArH), 1.75~1.79 (m, 1H, CH), 1.71~1.74 (m, 3H, CH₃), 1.23~1.30 (m, 3H, CH₃) ppm; ¹³C NMR (100 Hz, DMSO-*d*₆) δ : 174.63, 166.26, 156.49, 155.41, 139.74, 137.87, 131.73, 130.25, 129.71, 122.14, 51.39, 25.04, 23.45, 21.63, 20.88 ppm; ESI-MS: m/z : 460.7 [M-H]⁻.

4.1.8. Synthesis of quinoxaline-2,3(1*H*,4*H*)-dione (**7**)

A round-bottom flask charged with benzene-1,2-diamine (46.3 mmol, 5.0g) and oxalic acid (64.4 mmol, 5.8g), and 250 mL of distilled water was added in one portion. Then 4.5 mL of concentrated hydrochloric acid was added to the suspension dropwise and the reaction mixture was refluxed for 8h. Collected the obtained brown precipitate and washed with distilled water to afford 6.9 g of desired product, yield: 92%. M.p. 241~242.7 °C; ESI-MS m/z : 161.0 [M+H]⁺.

4.1.9. Synthesis of 2,3-dichloroquinoxaline (**8**)

A solution of compound **7** (30.84 mmol, 5.0g) in phosphorus oxychloride (30 mL) was reacted under refluxing condition for 5h, then the reaction was totally quenched by slowly pouring into cooled ammonia

solution. The mixture was extracted with ethyl acetate (2×50 mL), the combined organic phase was washed with brine (30 mL) and dried over anhydrous MgSO_4 . After evaporated in *vacuo*, the crude residue was purified by silica gel flash chromatography (PE/EtOAc=10:1, v:v) to give 4.9 g of corresponding product with 80% yield. M.p. 149–150 °C; ESI-MS m/z : 199.8 $[\text{M}+\text{H}]^+$.

4.1.10. Synthesis of methyl 4-((3-chloroquinoxalin-2-yl)oxy)benzoate (**9**)

Methyl 4-hydroxybenzoate (3.8 g, 25 mmol) and K_2CO_3 (4.1 g, 30 mmol) were dissolved in 150 mL of anhydrous DMF and the mixture was reacted at 85°C under nitrogen atmosphere. After 12h, compound **8** (4.98 g, 25 mmol) was added to the mixture in one portion and the reaction was allowed to react for additional 12h at the same temperature until completion, as determined by TLC. The reaction was then quenched by pouring into 250 mL of iced water and extracted with ethyl acetate (2 × 100 mL), the organic phase was then washed successively with 5% citric acid (2 × 75 mL), saturated NaHCO_3 (2 × 75 mL) and brine (2 × 50 mL). The combined organic solvent was removed under vacuum, and the crude residue was purified by flash chromatography (PE/EtOAc=50:1, v:v) to give 3.98 g of corresponding product as semi-solid with 50% yield. ESI-MS m/z : 315.3 $[\text{M}+\text{H}]^+$.

4.1.11. General procedure for the synthesis of methyl 4-((3-substituted quinoxalin-2-yl)oxy)benzoate (**10**)

Compound **9** (2.0 g, 6.4 mmol) was dissolved in 50 mL of anhydrous dimethyl sulfoxide, dodecyl amine (1.2 g, 6.5 mmol) and triethylamine (Et_3N , 1.5 g, 14.8 mmol) were added successively. The mixture was reacted at 75°C for 12h and quenched with 150 mL of iced water. It was then extracted with ethyl acetate (2 × 100 mL), washed with brine and dried over anhydrous Na_2SO_4 . Filtered and concentrated under vacuum condition, the crude residue was purified by flash chromatography (PE/EtOAc=100:1, v:v) to produce the corresponding product.

4.1.11.1. Methyl 4-((3-(dodecylamino)quinoxalin-2-yl)oxy)benzoate (**10a**). Semi-solid, yield 43%, ESI-MS m/z : 464.6 $[\text{M}+\text{H}]^+$.

4.1.11.2. Methyl 4-((3-(tert-butylamino)quinoxalin-2-yl)oxy)benzoate (**10b**). Semi-solid, yield 51%, ESI-MS m/z : 352.7 $[\text{M}+\text{H}]^+$.

4.1.12. General procedure for 4-((3-substituted quinoxalin-2-yl)oxy)benzoic acid (**11**)

These compounds were synthesized according to similar procedures with that of compound (**4**).

4.1.12.1. 4-((3-(Dodecylamino)quinoxalin-2-yl)oxy)benzoic acid (**11a**). Semi-solid, yield 88%, ESI-MS m/z : 448.7 $[\text{M}-\text{H}]^-$.

4.1.12.2. 4-((3-(tert-Butylamino)quinoxalin-2-yl)oxy)benzoic acid (**11b**). Semi-solid, yield 84%, ESI-MS m/z : 336.5 $[\text{M}-\text{H}]^-$.

4.1.13. General procedure for the synthesis of (R)-substituted 2-(4-((3-(substitutedamino)quinoxalin-2-yl)oxy)benzamido)propanoate (**12**)

Compound **11a** (0.45 mmol, 0.2 g) was dissolved in anhydrous THF (15 mL), then isobutyl chloroformate (0.83 mmol, 107 μL) and *N*-methylmorpholine (0.85 mmol, 93 μL) were added successively.

The temperature was maintained below -5°C in an ice-salt bath for 30 min. After the addition of L-phenylalanine methyl ester hydrochloride (0.6 mmol, 120 mg) was added in several portions, the mixture was allowed to warm to room temperature and stirred for another 4h under nitrogen atmosphere. The solvent was removed under vacuum and partitioned between EtOAc (2×50 mL) and saturated NH_4Cl solution. The organic phase was separated and washed with saturated NaHCO_3 (2×50 mL) and then with brine (50 mL), dried over anhydrous MgSO_4 , filtered, and concentrated in *vacuo* to give the crude product, which was further purified by flash chromatography (PE/EtOAc=25:1, v:v) to generate the pure product.

4.1.13.1. (S)-Methyl 2-(4-((3-(dodecylamino)quinoxalin-2-yl)oxy)benzamido)-3-phenylpropanoate (12a).

White solid, yield 68%, m.p. = $155\sim 157^{\circ}\text{C}$; ^1H NMR (400 MHz, CDCl_3) δ : 7.82~7.84 (d, $J = 8.7$ Hz, 2H, ArH), 7.68~7.70 (d, $J = 9.2$ Hz, 1H, ArH), 7.50~7.52 (d, $J = 7.0$ Hz, 1H, ArH), 7.42~7.46 (t, $J = 7.7$ Hz, 1H, ArH), 7.33~7.35 (d, $J = 8.7$ Hz, 2H, ArH), 7.25~7.33 (dd, $J_1 = 14.2$ Hz, $J_2 = 5.1$ Hz, 4H, ArH), 7.15~7.17 (d, $J = 8.1$ Hz, 2H, ArH), 6.59~6.61 (d, $J = 7.6$ Hz, 1H, $\text{NH}-\text{C}=\text{O}$), 5.58~5.61 (t, $J = 5.4$ Hz, 1H, NHCH_2), 5.09~5.14 (m, 1H, $\text{CH}-\text{C}=\text{O}$), 3.67 (s, 3H, OCH_3), 3.62~3.65 (m, 2H, NHCH_2), 3.22~3.33 (m, 2H, CH_2Ph), 1.24~1.28 (m, 20H, $(\text{CH}_2)_{10}$), 0.86~0.90 (t, $J = 7.0$ Hz, 3H, CH_3) ppm; ^{13}C NMR (100 MHz, CDCl_3) δ : 172.06, 171.16, 166.10, 155.30, 147.37, 144.72, 140.15, 135.82, 134.20, 131.02, 129.36, 128.70, 128.68, 127.56, 127.27, 126.90, 125.43, 124.20, 121.91, 60.40, 53.59, 52.49, 41.03, 37.94, 31.92, 29.64, 29.59, 29.41, 29.36, 27.14, 22.70, 21.06, 14.21, 14.13 ppm; ESI-MS m/z : 611.6 $[\text{M}+\text{H}]^+$.

4.1.13.2. (S)-Methyl 2-(4-((3-(dodecylamino)quinoxalin-2-yl)oxy)benzamido)propanoate (12b). White solid, yield 52%, m.p. = $143\sim 144^{\circ}\text{C}$; ^1H NMR (400 MHz, CDCl_3) δ : 8.93 (m, 1H, NH), 8.01~8.06 (m, 2H, ArH), 7.93 (m, 1H, ArH), 7.47~7.49 (d, $J = 8.0$ Hz, 3H, ArH), 7.40~7.44 (m, 1H, ArH), 7.29~7.32 (t, $J = 8.0$ Hz, 1H, ArH), 3.64 (s, 3H, OCH_3), 3.40~3.43 (m, 1H, $\text{CHC}=\text{O}$), 1.66~1.70 (m, 2H, NHCH_2), 1.35~1.40 (m, 3H, $\text{NHCH}(\text{CH}_3)$), 1.20~1.30 (m, 20H, $(\text{CH}_2)_{10}$), 0.80~0.83 (m, 3H, CH_2CH_3) ppm; ^{13}C NMR (100 MHz, CDCl_3) δ : 173.84, 166.19, 155.45, 147.57, 144.88, 140.32, 134.40, 131.27, 128.83, 127.69, 127.06, 125.60, 124.34, 122.08, 52.78, 48.73, 41.18, 32.07, 29.82, 29.79, 29.74, 29.56, 29.50, 27.30, 22.84, 18.89, 14.26 ppm; ESI-MS m/z : 535.5 $[\text{M}+\text{H}]^+$.

4.1.13.3. (2S,3R)-Methyl 2-(4-((3-(dodecylamino)quinoxalin-2-yl)oxy)benzamido)-3-methyl pentanoate (12c). White solid, yield 50%, m.p. = $166\sim 167^{\circ}\text{C}$; ^1H NMR (400 MHz, CDCl_3) δ : 7.90~7.92 (d, $J = 8.0$ Hz, 2H, ArH), 7.68~7.70 (d, $J = 8.0$ Hz, 1H, ArH), 7.50~7.52 (d, $J = 8.0$ Hz, 2H, ArH), 7.42~7.46 (t, $J = 6.0$ Hz, 1H, ArH), 7.36~7.38 (d, $J = 6.0$ Hz, 2H, ArH), 6.66~6.68 (d, $J = 6.0$ Hz, 1H, $\text{NH}-\text{C}=\text{O}$), 5.60 (m, 1H, NHCH_2), 4.83~4.87 (m, 1H, $\text{CH}-\text{C}=\text{O}$), 3.80 (s, 3H, OCH_3), 3.63~3.68 (m, 2H, NHCH_2), 2.00~2.08 (m, 1H, $\text{NHCHCH}_2\text{CH}_3$), 1.74~1.76 (m, 2H, CHCH_2CH_3), 1.30~1.41 (m, 20H, $(\text{CH}_2)_{10}$), 0.97~1.01 (t, 6H, $J = 6.0$ Hz, $2 \times \text{CH}_3$) ppm; ^{13}C NMR (100 MHz, CDCl_3) δ : 172.79, 166.50, 155.42, 147.57, 144.88, 134.41, 131.50, 128.83, 127.69, 127.08, 125.61, 124.34, 122.10, 57.02, 52.38, 41.19, 38.50, 32.07, 29.79, 29.74, 29.56, 29.50, 27.30, 25.59, 22.84, 15.70, 14.26, 11.79 ppm; ESI-MS m/z : 577.8 $[\text{M}+\text{H}]^+$.

4.1.13.4. Methyl 2-(4-((3-(tert-butylamino)quinoxalin-2-yl)oxy)benzamido)acetate (12d). White solid, yield

62%, m.p. = 172–173°C; ^1H NMR (400 MHz, CDCl_3) δ : 7.90–7.93 (m, 2H, ArH), 7.67–7.69 (d, J = 8.0 Hz, 1H, ArH), 7.47–7.51 (t, J = 8.0 Hz, 2H, ArH), 7.29–7.43 (m, 3H, ArH), 6.72 (m, 1H, C=O-NH), 5.53 (s, 1H, N=C-NH), 4.28–4.29 (d, J = 4.0 Hz, 2H, $\text{NHCH}_2\text{C=O}$), 3.83 (s, 3H, OCH_3), 1.25–1.34 (m, 9H, $(\text{CH}_3)_3$) ppm; ^{13}C NMR (100 MHz, CDCl_3) δ : 170.56, 166.78, 155.93, 148.46, 145.93, 139.92, 134.61, 130.27, 128.73, 127.57, 126.42, 125.62, 124.54, 121.56, 52.53, 44.77, 41.80, 13.79 ppm; ESI-MS m/z : 409.7 $[\text{M}+\text{H}]^+$.

4.1.13.5. (*S*)-Methyl 2-(4-((3-(*tert*-butylamino)quinoxalin-2-yl)oxy)benzamido)propanoate (**12e**). White solid, yield 65%, m.p. = 177–178°C; ^1H NMR (400 MHz, CDCl_3) δ : 7.90–7.94 (t, J = 8.0 Hz, 2H, ArH), 7.68–7.70 (d, J = 8.0 Hz, 1H, ArH), 7.31–7.37 (m, 3H, ArH), 7.42–7.52 (m, 2H, ArH), 6.81–6.82 (d, J = 4.0 Hz, 1H, C=O-NH), 4.81–4.88 (m, 1H, NHCHC=O), 3.82 (s, 3H, OCH_3), 3.74–3.79 (m, 1H, N=C-NH), 1.55–1.63 (m, 9H, $(\text{CH}_3)_3$), 1.31–1.35 (m, 3H, CH_3) ppm; ^{13}C NMR (100 MHz, CDCl_3) δ : 164.71, 155.51, 147.42, 143.81, 139.87, 133.67, 130.52, 128.90, 127.38, 126.59, 125.85, 124.12, 122.15, 121.65, 52.02, 44.80, 28.73, 18.05, 13.78 ppm; ESI-MS m/z : 433.5 $[\text{M}+\text{H}]^+$.

4.1.13.6. (2*S*,3*R*)-Methyl 2-(4-((3-(*tert*-butylamino)quinoxalin-2-yl)oxy)benzamido)-3-methyl pentanoate (**12f**). White solid, yield 51%, m.p. = 166–167°C; ^1H NMR (400 MHz, CDCl_3) δ : 7.82–7.84 (d, J = 8.6 Hz, 2H, ArH), 7.58–7.61 (d, J = 8.2 Hz, 1H, ArH), 7.39–7.41 (d, J = 7.0 Hz, 1H, ArH), 7.32–7.35 (t, J = 7.0 Hz, 1H, ArH), 7.24–7.28 (t, J = 7.5 Hz, 2H, ArH), 7.13–7.18 (m, 1H, ArH), 6.65–6.67 (d, J = 8.2 Hz, 1H, NHCHC=O), 5.46 (s, 1H, NHCHCH_3), 4.75–4.78 (m, 1H, CHCHC=O), 3.70 (s, 3H, OCH_3), 1.58 (s, 9H, $(\text{CH}_3)_3$), 1.22–2.25 (t, J = 6.9 Hz, 2H, CHCHCH_2), 1.17 (m, 1H, CHCHCH_2), 0.88–0.92 (m, 6H, $2\times\text{CH}_3$) ppm; ^{13}C NMR (100 MHz, CDCl_3) δ : 172.70, 166.43, 155.29, 147.41, 143.84, 139.88, 133.82, 131.21, 128.69, 127.32, 126.80, 125.80, 124.06, 122.05, 56.89, 52.27, 52.00, 38.28, 28.76, 25.42, 15.56, 11.66 ppm; ESI-MS m/z : 465.8 $[\text{M}+\text{H}]^+$.

4.1.13.7. (*S*)-Methyl 2-(4-((3-(*tert*-butylamino)quinoxalin-2-yl)oxy)benzamido)-4-methylpentanoate (**12g**). White solid, yield 58%, m.p. = 170–172°C; ^1H NMR (400 MHz, CDCl_3) δ : 7.80–7.83 (t, J = 5.8 Hz, 2H, ArH), 7.57–7.59 (dd, J_1 = 8.2 Hz, J_2 = 0.9 Hz, 1H, ArH), 7.38–7.40 (dd, J_1 = 8.0 Hz, J_2 = 0.9 Hz, 1H, ArH), 7.31–7.34 (t, J = 7.6 Hz, 1H, ArH), 7.21–7.24 (m, 2H, ArH), 7.12–7.17 (m, 1H, ArH), 6.72–6.74 (d, J = 6.3 Hz, 1H, C=ONH), 5.45 (s, 1H, N=C-NH), 4.77–4.82 (m, 1H, NHCHC=O), 3.69 (s, 3H, OCH_3), 1.62 (d, J = 2.9 Hz, 1H, $\text{CH}_2\text{CH}(\text{CH}_3)_2$), 1.55 (m, 9H, $(\text{CH}_3)_3$), 1.21 (m, 2H, CHCH_2CH), 0.90 (m, 6H, $2\times\text{CH}_3$) ppm; ^{13}C NMR (100 MHz, CDCl_3) δ : 173.90, 166.48, 155.29, 147.43, 143.84, 139.87, 133.84, 130.96, 128.77, 127.30, 126.78, 125.80, 124.06, 122.00, 52.45, 52.29, 51.24, 41.73, 28.76, 25.03, 22.92, 22.03 ppm; ESI-MS m/z : 465.6 $[\text{M}+\text{H}]^+$.

4.1.13.8. (*S*)-Methyl 2-(4-((3-(*tert*-butylamino)quinoxalin-2-yl)oxy)benzamido)-3-phenylpropanoate (**12h**). White solid, yield 65%, m.p. = 182–183°C; ^1H NMR (400 MHz, CDCl_3) δ : 7.73–7.76 (t, J = 6.9 Hz, 2H, ArH), 7.59–7.61 (d, J = 8.2 Hz, 1H, ArH), 7.40–7.43 (dd, J_1 = 11.0 Hz, J_2 = 3.1 Hz, 1H, ArH), 7.33–7.37 (m, 1H, ArH), 7.16–7.27 (m, 6H, ArH), 7.07–7.09 (d, J = 6.9 Hz, 2H, ArH), 6.53–6.55 (d, J = 6.0 Hz, 1H,

NH-C=O), 5.42~5.48 (m, 1H, N=C-NH), 5.02~5.07 (m, 1H, NHCHC=O), 3.71 (s, 3H, OCH₃), 3.16~3.27 (m, 2H, CH₂C₆H₅), 1.22~1.54 (m, 9H, (CH₃)₃) ppm; ¹³C NMR (100 MHz, CDCl₃) δ: 171.04, 165.09, 154.33, 146.29, 142.80, 138.83, 134.77, 132.74, 128.32, 127.62, 127.66, 126.30, 126.23, 125.75, 124.76, 123.03, 120.95, 120.49, 52.55, 51.47, 50.96, 36.89, 27.71 ppm; ESI-MS *m/z*: 499.1 [M+H]⁺.

4.1.14. General procedure for the preparation of (S)-2-(4-((3-substituted quinoxalin-2-yl)oxy)benzamido)-2-substituted acetic acid (**13a-h**).

The synthetic procedure of compound **13** was carried out according to that of compounds (**11a-b**).

4.1.14.1. (S)-2-(4-((3-(Dodecylamino)quinoxalin-2-yl)oxy)benzamido)-3-phenylpropanoic acid (**13a**). White crystal obtained from recrystallization (MeOH:H₂O = 3:1, v:v), yield 93%, m.p. = 139~141 °C; ¹H NMR (400 MHz, DMSO-*d*₆) δ: 8.60~8.61 (d, *J* = 6.0 Hz, 1H, O=C-NH), 7.89~7.91 (d, *J* = 7.9 Hz, 2H, ArH), 7.68 (s, 1H, NHCH₂), 7.53~7.55 (d, *J* = 7.9 Hz, 1H, ArH), 7.38~7.42 (m, 4H, ArH), 7.24~7.33 (m, 4H, ArH), 7.17~7.22 (dd, *J*₁ = 11.6 Hz, *J*₂ = 7.2 Hz, 2H ArH), 4.56 (s, 1H, NHCH₂COOH), 3.05~3.08 (m, 2H, NHCH₂), 1.66 (m, 2H, CH₂Ar), 1.23~1.34 (m, 20H, (CH₂)₁₀), 0.84 (m, 3H, CH₂CH₃) ppm; ¹³C NMR (100 MHz, DMSO-*d*₆) δ: 173.82, 166.09, 155.30, 148.46, 145.26, 140.30, 138.87, 133.95, 129.55, 129.49, 128.63, 127.63, 126.75, 123.88, 122.26, 55.01, 40.74, 36.87, 31.76, 29.53, 29.49, 29.28, 29.18, 27.03, 22.56, 14.40 ppm; ESI-MS *m/z*: 595.5 [M-H]⁻.

4.1.14.2. (S)-2-(4-((3-(Dodecylamino)quinoxalin-2-yl)oxy)benzamido)propanoic acid (**13b**). White crystal obtained from recrystallization (MeOH:H₂O = 3:1, v:v), yield 89%; m.p. = 179~180 °C; ¹H NMR (400 MHz, DMSO-*d*₆) δ: 12.46 (s, 1H, COOH), 8.75~8.73 (d, 1H, *J* = 6.0 Hz, CONH), 8.00~8.03 (d, *J* = 9.0 Hz, 2H, ArH), 7.64~7.68 (d, *J* = 12 Hz, 1H, ArH), 7.54~7.57 (d, *J* = 9.0 Hz, 1H, ArH), 7.38~7.46 (m, 3H, ArH), 7.19~7.24 (m, 1H, ArH), 4.43~4.47 (m, 1H, NHCH₂), 3.50~3.52 (m, 1H, CH), 1.67~1.71 (m, 3H, CHCH₂), 1.35~1.43 (m, 22H, (CH₂)₁₁), 0.82~0.87 (m, 3H, CH₂CH₃) ppm; ¹³C NMR (100 MHz, DMSO-*d*₆) δ: 175.38, 166.69, 156.08, 149.20, 146.04, 141.04, 134.70, 132.26, 130.31, 128.39, 127.46, 126.02, 124.65, 122.96, 49.39, 32.46, 30.23, 30.19, 30.15, 29.98, 29.87, 29.55, 27.73, 23.26, 18.10, 15.12 ppm; ESI-MS *m/z*: 519.6 [M-H]⁻.

4.1.14.3. (2S,3R)-2-(4-((3-(Dodecylamino)quinoxalin-2-yl)oxy)benzamido)-3-methylpentanoic acid (**13c**). White crystal obtained from recrystallization (MeOH:H₂O = 3:1, v:v), yield 92%; m.p. = 189~191 °C; ¹H NMR (400 MHz, DMSO-*d*₆) δ: 12.17 (s, 1H, COOH), 8.57~8.59 (d, *J* = 8.0 Hz, 1H, ArH), 8.02~8.04 (d, *J* = 8.6 Hz, 2H, ArH), 7.87 (s, 1H, C=ONH), 7.43~7.47 (m, 4H, ArH), 7.28~7.32 (t, *J* = 7.5 Hz, 1H, ArH), 4.33~4.37 (t, *J* = 7.5 Hz, 1H, CHC=O), 3.63 (m, 2H, NHCH₂), 1.98 (m, 1H, CH₃CHCH₂CH₃), 1.63~1.72 (m, 2H, CH₃CHCH₂CH₃), 1.23~1.38 (m, 20H, (CH₂)₁₀), 0.94~0.96 (d, *J* = 6.8 Hz, CH₂CH₂CH₃, 3H), 0.82~0.90 (m, 6H, 2×CH₃). ¹³C NMR (100 MHz, DMSO-*d*₆) δ: 173.69, 166.57, 154.90, 149.05, 132.99, 132.00, 129.94, 129.11, 128.36, 126.94, 125.06, 122.16, 57.80, 36.11, 31.78, 29.56, 29.47, 29.29, 29.06, 28.52, 26.83, 25.60, 22.58, 16.16, 14.44, 11.53 ppm; ESI-MS *m/z*: 561.5 [M-H]⁻.

4.1.14.4. 2-(4-((3-(tert-Butylamino)quinoxalin-2-yl)oxy)benzamido)acetic acid (**13d**). White crystal

obtained from recrystallization (MeOH:H₂O = 3:1, v:v), yield 86%; m.p. = 158~161 °C; ¹H NMR (400 MHz, DMSO-*d*₆) δ: 8.64 (s, 1H, C=ONHCH₂), 7.74~7.76 (d, *J* = 8.1 Hz, 2H, ArH), 7.33~7.37 (d, *J* = 14.6 Hz, 1H, ArH), 7.16~7.22 (m, 4H, ArH), 7.00~7.04 (m, 1H, ArH), 3.70~3.72 (d, *J* = 5.2 Hz, 2H, NHCH₂COOH), 2.26 (s, 1H, N=C-NHC(CH₃)₃), 1.04~1.33 (m, 9H, 3×CH₃) ppm; ¹³C NMR (100 MHz, DMSO-*d*₆) δ: 171.86, 166.31, 155.49, 149.10, 146.04, 139.70, 134.54, 131.29, 129.49, 127.98, 126.43, 125.66, 124.94, 122.03, 44.71, 28.80, 14.05 ppm; ESI-MS *m/z*: 393.2 [M-H][−].

4.1.14.5. (*S*)-2-(4-((3-(*tert*-Butylamino)quinoxalin-2-yl)oxy)benzamido)propanoic acid (**13e**). White crystal obtained from recrystallization (MeOH:H₂O = 3:1, v:v), yield 90%; m.p. = 135~137 °C; ¹H NMR (400 MHz, DMSO-*d*₆) δ: 8.73 (s, 1H, NHC=O), 7.99~8.02 (t, *J* = 8.0 Hz, 2H, ArH), 7.58~7.60 (d, *J* = 8.0 Hz, 1H, ArH), 7.41~7.44 (m, 4H, ArH), 7.24 (m, 1H, ArH), 4.43 (s, 1H, N=C-NHC(CH₃)₃), 3.72 (m, 1H, NHCHCOOH), 1.58 (m, 9H, 3×CH₃), 1.42 (m, 3H, CHCH₃) ppm; ¹³C NMR (100 MHz, DMSO-*d*₆) δ: 175.47, 166.53, 155.94, 149.07, 145.21, 140.42, 134.44, 132.40, 130.22, 128.83, 127.44, 126.43, 125.05, 123.08, 122.59, 51.83, 42.64, 29.96, 18.35 ppm; ESI-MS *m/z*: 407.5 [M-H][−].

4.1.14.6. (2*S*,3*R*)-2-(4-((3-(*tert*-Butylamino)quinoxalin-2-yl)oxy)benzamido)-3-methylpentanoic acid (**13f**). White crystal obtained from recrystallization (MeOH:H₂O = 3:1, v:v), yield 80%; m.p. = 154~156 °C; ¹H NMR (400 MHz, DMSO-*d*₆) δ: 12.52 (s, 1H, COOH), 8.37~8.39 (d, *J* = 8.0 Hz, 1H, NHCHCOOH), 7.98~8.00 (d, *J* = 8.0 Hz, 2H, ArH), 7.57~7.59 (d, *J* = 8.0 Hz, 1H, ArH), 7.38~7.44 (m, 4H, ArH), 7.22~7.26 (m, 1H, ArH), 6.60 (s, 1H, N=C-NHC(CH₃)₃), 4.27~4.30 (s, 1H, CHC=O), 1.91~1.96 (m, 1H, NHCHCOOH), 1.49~1.58 (m, 9H, 3×CH₃), 1.23~1.32 (m, 2H, CH₂), 0.80~0.94 (m, 6H, 2×CH₃) ppm; ¹³C NMR (100 MHz, DMSO-*d*₆) δ: 154.32, 148.37, 144.00, 139.64, 133.99, 132.03, 129.70, 127.66, 126.69, 125.53, 122.02, 58.03, 51.41, 36.43, 28.76, 25.44, 16.78, 13.39, 11.43 ppm; ESI-MS *m/z*: 449.4 [M-H][−].

4.1.14.7. (*S*)-2-(4-((3-(*tert*-Butylamino)quinoxalin-2-yl)oxy)benzamido)-4-methylpentanoic acid (**13g**). White crystal obtained from recrystallization (MeOH:H₂O = 3:1, v:v), yield 81%; m.p. = 177~178 °C; ¹H NMR (400 MHz, DMSO-*d*₆) δ: 12.44 (s, 1H, COOH), 8.51~8.53 (d, *J* = 8.0 Hz, 1H, C=ONHCHCOOH), 7.99~8.01 (d, *J* = 8.0 Hz, 2H, ArH), 7.57~7.59 (d, 1H, *J* = 8.0 Hz, ArH), 7.38~7.44 (m, 4H, ArH), 7.21~7.25 (m, 1H, ArH), 6.59 (s, 1H, N=C-NHC(CH₃)₃), 4.40 (s, 1H, CHC=O), 1.72~1.77 (m, 2H, CH₂), 1.48~1.64 (m, 9H, 3×CH₃), 1.23~1.29 (m, 1H, CH), 0.83~0.93 (m, 6H, 2×CH₃) ppm; ¹³C NMR (100 MHz, DMSO-*d*₆) δ: 165.87, 155.09, 144.46, 139.65, 133.69, 131.66, 131.36, 129.42, 127.64, 125.67, 124.31, 122.37, 52.10, 28.83, 25.10, 23.58, 21.94 ppm; ESI-MS *m/z*: 449.4 [M-H][−].

4.1.14.8. (*S*)-2-(4-((3-(*tert*-Butylamino)quinoxalin-2-yl)oxy)benzamido)-3-phenylpropanoic acid (**13h**). White crystal obtained from recrystallization (MeOH:H₂O = 3:1, v:v), yield 84%; m.p. = 168~180 °C; ¹H NMR (400 MHz, DMSO-*d*₆) δ: 8.28 (s, 1H, NH), 7.87~7.89 (d, *J* = 6.5 Hz, 2H, ArH), 7.57~7.61 (d, *J* = 7.9 Hz, 1H, ArH), 7.36~7.46 (m, 4H, ArH), 7.23~7.28 (m, 5H, ArH), 7.14~7.16 (d, *J* = 6.8 Hz, 1H, ArH), 4.49 (s, 1H, CHC=O), 3.70~3.72 (d, *J* = 8.0 Hz, 2H, CH₂Ar), 3.08 (s, 1H, N=C-NHC(CH₃)₃), 1.25~1.57 (m, 9H, 3×CH₃) ppm; ¹³C NMR (100 MHz, DMSO-*d*₆) δ: 173.87, 165.89, 160.99, 155.23, 148.36, 144.46, 139.66,

134.53, 133.65, 131.34, 130.21, 129.54, 129.41, 128.66, 127.70, 126.80, 125.69, 124.33, 122.44, 60.24, 52.11, 36.83, 28.80 ppm; ESI-MS m/z : 483.1 [M-H].

4.2. Biological protocols

4.2.1. *In vitro* anti-proliferative assay

The tested chemicals were dissolved in dimethylsulfoxide (DMSO) or PBS and diluted to the desired concentration with culture medium before using. The cell lines were maintained in RPMI-1640 medium supplemented with 10% (v/v) heat-inactivated fetal bovine serum (FBS) and incubated at 37°C in a humidified incubator with 5% CO₂. Cell proliferation was determined by the MTT (3-[4,5-dimethyl-2-thiazolyl]-2,5-diphenyl-2H-tetrazolium bromide) method. Briefly, cells were seeded in a 96-well plate (10⁴ cells per well). After 4 h incubation, chemicals were subsequently added to wells to achieve final concentration of 200, 150, 100, 50, and 10 μM. Control wells were prepared by addition of culture medium. Treated cells were then incubated for 48 h. Once completion of incubation, 1% of 0.5 mg/mL MTT solution was added to each well and incubated for an additional 4 h. Formazan formed from MTT was extracted by adding 100 μL of DMSO and mixed for another 15 min. The optical density was measured using an enzyme-linked immunosorbent assay (ELISA) reader (Model 680, BIO-RAD) at 570 nm.

The growth inhibition rate was calculated as $[(OD_c - OD_t) / (OD_c - OD_z)] \times 100\%$. In this formula, OD_c represents the OD values of the control group, OD_t represents the OD values of the treating groups, and OD_z represents the OD values of the zero-setting groups. Three independent experiments with triplicated samples were performed to achieve the cytotoxic results, and the IC₅₀ values were calculated according to inhibition ratios.

4.2.2. *In vivo* anti-metastatic experiment

Preparation of solution: Tested compounds were dissolved in 0.5% CMC-Na to prepare solution or homogeneous suspension, with a final concentration of 2 mg/ml. If possible, ultrasonic device can be utilized to promote dissolution.

Experimental animal model and grouping: Ascites was drawn from BALB/c mice bearing with hepatocarcinoma 22 (H22) under aseptic condition, and diluted with physiological saline at 1:4. Final concentration of tumor cells was 3 × 10⁷ cells/ml. Then 50 healthy BALB/c mice weighing 18–22 g were selected (available from Laboratory Animal Center, Shandong University), and 0.2 mL of hepatoma H22 cell suspension (6 × 10⁶ cells) were inoculated *via* the caudal vein of the mice. After 24h, they were weighted and randomly divided into 7 groups, 10 mice in each group (bisexual each half).

Drug dosages and methods: Animals of treatment groups were given tested compounds (**6b**, **6g**, **13a**, **13b**, **13f** and positive control Doxo) through intragastric administration, while the control group (0.5% CMC-Na as a blank) was treated with the same volume of excipient by intragastric route, at a dose of 10

mg/kg/day, 6 days/week for two consecutive weeks. On the twelfth day, all the surviving mice were weighed and sacrificed for autopsy immediately. Lungs, livers, spleen with tumor nodes were removed and weighed. Then lungs were placed in Bouin's stationary solution (saturated 2,4,6-trinitrophenol solution/formaldehyde/glacial acetic acid = 15:5:1). One day later, the number of metastasized nodes on lung surface was counted under a microscope. The inhibitory rate (%) was calculated according to the following formula:

$$\text{Inhibitory rate (\%)} = \{[(\text{the average number of metastasized nodes of the control group}) - (\text{the average number of metastasized nodes of the experimental group})] / (\text{the average number of metastasized nodes of control group})\} \times 100\%.$$

4.3. Statistical analysis

Statistical significance was determined by the Student's *t*-test after one-way ANOVA, without correction for multiple comparisons. The limit of statistical significance was $p < 0.05$.

4.4. Topo II-mediated kDNA decatenation assay

Reaction buffer solution contains 50 mM tris(hydroxymethyl)aminomethane (Tris-HCl, pH 8.0), 0.5 mM dithiothreitol (DTT), 10 mM MgCl₂, 2 mM ATP, and 20 μg/mL kDNA. Human topo IIα, 0.5 units (TopoGen, TG2000H), was added right before the reaction. Indicated amount of tested compounds were included in 20 μL of topo II reaction buffer. Mixtures were incubated for 15 min at 37°C, and then stopped by adding 3 μL of stop solution containing 5% of SDS and 50% of glycerol. Electrophoresis was used to separate the reaction products by running 1% agarose gel at 50 V for 50 minutes. Ethidium bromide-stained DNA was visualized under UV light.

4.5. Molecular modeling procedure

The docking experiment was carried out based on the X-ray structure of topo IIα (PDB code: 1ZXM) [45] and performed as follows: Selected compounds **XK469** and **13b** were constructed with a Sybyl/Sketch module and optimized using Powell Energetic Gradient method with a Tripos force field with the convergence criterion set at 0.05 kcal/mol·Å, and assigned with Gasteiger-Hückel method. In this crystal structure, Mg²⁺ ion and its two binding water molecules (W924, W931) were retained since it was assumed that they played important roles in molecular recognition [46], and other docking parameters implied in the program were kept as default.

Acknowledgment

This work was financially supported by the Natural Science Foundation of Shandong Province (No. ZR2013HM101), China–Australia Centre for Health Sciences Research Program (No. 2015GJ07), “ChangJiang Scholars and Innovative Research Team in University” Program (PCSIRT, No. IRT13028), and also Shandong Innovation and Transformation of Achievements Grant (No. 2014ZZCX02601).

References

- [1] S.D. Undevia, F. Innocenti, J. Ramirez, L. House, A.A. Desai, L.A. Skoog, D.A. Singh, T. Karrison, H.L. Kindler, M.J. Ratain, A phase I and pharmacokinetic study of the quinoxalineantitumour agent R(+)-XK469 in patients with advanced solid tumours. *Eur. J. Cancer.* 12 (2008) 1684–1692.
- [2] W. Stock, S.D. Undevia, C. Bivins, F. Ravandi, O. Odenike, S. Faderl, E. Rich, G. Borthakur, L. Godley, S. Verstovsek, A. Artz, W. Wierda, R.A. Larson, Y. Zhang, J. Cortes, M.J. Ratain, F.J. Giles, A phase I and pharmacokinetic study of XK469R (NSC 698215), a quinoxaline phenoxypropionic acid derivative, in patients with refractory acute leukemia. *Invest. New Drugs.* 26 (2008) 331–338.
- [3] Z. Ding, R.E. Parchment, P.M. LoRusso, J.Y. Zhou, J. Li, T.S. Lawrence, Y. Sun, G.S. Wu, The investigational new drug XK469 induces G(2)-M cell cycle arrest by p53-dependent and -independent pathways. *Clin. Cancer Res.* 7 (2001) 3336–3342.
- [4] Z. Ding, J.Y. Zhou, W.Z. Wei, V.V. Baker, G.S. Wu, Induction of apoptosis by the new anticancer drug XK469 in human ovarian cancer cell lines. *Oncogene.* 21 (2002) 4530–4538.
- [5] H. Lin, B. Subramanian, A. Nakeff, B.D. Chen, XK469, a novel antitumor agent, inhibits signaling by the MEK/MAPK signaling pathway. *Cancer Chemother. Pharmacol.* 49 (2002) 281–286.
- [6] H. Lin, X.Y. Liu, B. Subramanian, A. Nakeff, F. Valeriote, B.D. Chen, Mitotic arrest induced by XK469, a novel antitumor agent, is correlated with the inhibition of cyclin B1 ubiquitination. *Int. J. Cancer.* 97 (2002) 121–128.
- [7] D. Kessel, J.J. Jr. Reiners, S.T. Hazeldine, L. Polin, J.P. Horwitz, The role of autophagy in the death of L1210 leukemia cells initiated by the new antitumor agents, XK469 and SH80. *Mol. Cancer Ther.* 6 (2007) 370–379.
- [8] H. Gao, K.C. Huang, E.F. Yamasaki, K.K. Chan, L. Chohan, R.M. Snapka, XK469, a selective topoisomerase II beta poison. *Proc. Natl. Acad. Sci. U S A.* 96 (1999) 12168–12173.
- [9] A.M. Alousi, R. Boinpally, R. Wiegand, R. Parchment, S. Gadgeel, L.K. Heilbrun, A.J. Wozniak, P. DeLuca, P.M. LoRusso, A phase 1 trial of XK469: toxicity profile of a selective topoisomerase II beta inhibitor. *Invest. New Drugs.* 25 (2007) 147–154.
- [10] E.J. Mensah-Osman, A.M., Al-Katib H.Y. Wu, N.I. Osman, R.M. Mohammad, 2-[4-(7-chloro-2-quinoxalinyloxyphenoxy)-propionic acid (XK469), an inhibitor of topoisomerase (Topo) II beta, up-regulates Topo II alpha and enhances Topo II alpha-mediated cytotoxicity. *Mol. Cancer Ther.* 1 (2002) 1321–1326.
- [11] S.T. Hazeldine, L. Polin, J. Kushner, J. Paluch, K. White, M. Edelstein, E. Palomino, T.H. Corbett, J.P. Horwitz, Design, synthesis, and biological evaluation of analogues of the antitumor agent, 2-(4-[(7-chloro-2-quinoxalinyloxy)phenoxy]propionic acid (XK469). *J. Med. Chem.* 44 (2001) 1758–1776.
- [12] S.T. Hazeldine, L. Polin, J. Kushner, K. White, N.M. Bouregeois, B. Crantz, E. Palomino, T.H. Corbett, J.P. Horwitz, II. Synthesis and biological evaluation of some bioisosteres and congeners of the antitumor agent, 2-(4-[(7-chloro-2-quinoxalinyloxy)phenoxy]propionic acid (XK469). *J. Med. Chem.* 45 (2002) 3130–3137.

- [13] S.T. Hazeldine, L. Polin, J. Kushner, K. White, T.H. Corbett, J. Biehl, J.P. Horwitz, Part 3: synthesis and biological evaluation of some analogs of the antitumor agents, 2-{4-[(7-chloro-2-quinoxalinyloxy]phenoxy}propionic acid, and 2-{4-[(7-bromo-2-quinolinyloxy]phenoxy}propionic acid. *Bioorg. Med. Chem.* 13 (2005) 1069–1081.
- [14] S.T. Hazeldine, L. Polin, J. Kushner, K. White, T.H. Corbett, J.P. Horwitz, Synthetic modification of the 2-oxypropionic acid moiety in 2-{4-[(7-chloro-2-quinoxalinyloxy]phenoxy}propionic acid (XK469), and consequent antitumor effects. Part 4. *Bioorg. Med. Chem.* 13 (2005) 3910–3920.
- [15] S.T. Hazeldine, L. Polin, J. Kushner, K. White, T.H. Corbett, J.P. Horwitz, Synthesis and biological evaluation of conformationally constrained analogs of the antitumor agents XK469 and SH80. Part 5. *Bioorg. Med. Chem.* 14 (2006) 2462–2467.
- [16] A.K. Ghosh, D.D. Anderson, I.T. Weber, H. Mitsuya, Enhancing protein backbone binding--a fruitful concept for combating drug-resistant HIV. *Angew. Chem. Int. Ed. Engl.* 51 (2012) 1778–1802.
- [17] A.T. Baviskar, C. Madaan, R. Preet, P. Mohapatra, V. Jain, A. Agarwal, S.K. Guchhait, C.N. Kundu, U.C. Banerjee, P.V. Bharatam, N-fused imidazoles as novel anticancer agents that inhibit catalytic activity of topoisomerase II α and induce apoptosis in G1/S phase. *J. Med. Chem.* 54 (2011) 5013–5030.
- [18] L. Jiang, L. Lai, CH...O hydrogen bonds at protein-protein interfaces. *J. Biol. Chem.* 277 (2002) 37732–37740.
- [19] P. Chène, J. Rudloff, J. Schoepfer, P. Furet, P. Meier, Z. Qian, J.M. Schlaeppli, R. Schmitz, T. Radimerski, Catalytic inhibition of topoisomerase II by a novel rationally designed ATP-competitive purine analogue. *BMC. Chem. Biol.* 9 (2009) 1.
- [20] P. Furet, J. Schoepfer, T. Radimerski, P. Chène, Discovery of a new class of catalytic topoisomerase II inhibitors targeting the ATP-binding site by structure based design. Part I. *Bioorg. Med. Chem. Lett.* 19 (2009) 4014–4017.
- [21] (a) Y.R. Zheng, K. Suntharalingam, T.C. Johnstone, H. Yoo, W. Lin, J.G. Brooks, S.J. Lippard, Pt(IV) prodrugs designed to bind non-covalently to human serum albumin for drug delivery. *J. Am. Chem. Soc.* 136 (2014) 8790–8798; (b) D. Dong, Z. Li, X. Li, Z. Li, Recombinant human serum albumin fusion proteins: novel applications and challenges. Chapter 3, pp 47-68, 2015. NOVA Publishers. New York.
- [22] M. Li, S. Qi, Y. Jin, W. Yao, S. Zhang, J. Zhao, Amphiphilic lipid derivatives of 3'-hydroxyurea-deoxythymidine: preparation, properties, molecular self-assembly, simulation and *in vitro* anticancer activity. *Colloids. Surf. B. Biointerfaces.* 123 (2014) 852–858.
- [23] J.A. Menendez, L. Vellon, R. Lupu, DNA topoisomerase II alpha (TOP2A) inhibitors up-regulate fatty acid synthase gene expression in SK-Br3 breast cancer cells: *in vitro* evidence for a 'functional amplicon' involving FAS, Her-2/neu and TOP2A genes. *Int. J. Mol. Med.* 18 (2006) 1081–1087.

- [24] J.P. Nam, S.C. Park, T.H. Kim, J.Y. Jang, C. Choi, M.K. Jang, J.W. Nah, Encapsulation of paclitaxel into lauric acid-O-carboxymethyl chitosan-transferrin micelles for hydrophobic drug delivery and site-specific targeted delivery. *Int. J. Pharm.* 457 (2013) 124–135.
- [25] S. Jubie, P. Dhanabal, M. Afzal Azam, N. Muruganantham, R. Kalirajan, K. Elango, Synthesis and characterization of some novel fatty acid analogues: a preliminary investigation on their activity against human lung carcinoma cell line. *Lipids Health Dis.* 12 (2013) 45.
- [26] Y. Mizushima, T. Tsuzuki, T. Eitsuka, T. Miyazawa, K. Kobayashi, H. Ikawa, I. Kuriyama, Y. Yonezawa, M. Takemura, H. Yoshida, K. Sakaguchi, Inhibitory action of conjugated C18-fatty acids on DNA polymerases and DNA topoisomerases. *Lipids.* 39 (2004) 977–983.
- [27] J.A. Menendez, R. Lupu, Fatty acid synthase-catalyzed de novo fatty acid biosynthesis: from anabolic-energy-storage pathway in normal tissues to jack-of-all-trades in cancer cells. *Arch. Immunol. Ther. Exp (Warsz).* 52 (2004) 414–426.
- [28] Y.A. Hannun, L.M. Obeid, The ceramide-centric universe of lipid-mediated cell regulation: stress encounters of the lipid kind. *J. Biol. Chem.* 277 (2002) 25847–25850.
- [29] L. Yang, P. Wang, J.F. Wu, L.M. Yang, R.R. Wang, W. Pang, Y.G. Li, Y.M. Shen, Y.T. Zheng, X. Li, Design, synthesis and anti-HIV-1 evaluation of hydrazide-based peptidomimetics as selective gelatinase inhibitors. *Bioorg Med Chem.* 24 (2016) 2125–2136.
- [30] L. Shi, J. Zhou, J. Wu, J. Cao, Y. Shen, H. Zhou, X. Li, Quinoxalinone (Part II). Discovery of (Z)-3-(2-(pyridin-4-yl)vinyl)quinoxalinone derivatives as potent VEGFR-2 kinase inhibitors. *Bioorg. Med. Chem.* 24 (2016) 1840–1852.
- [31] X. Li, J. Taechalertrapisarn, D. Xin, K. Burgess, Protein-protein interface mimicry by an oxazoline piperidine-2,4-dione. *Org. Lett.* 17 (2015) 632–635.
- [32] L. Shi, Q. Wang, H. Wang, H. Zhou, Y. Li, X. Li, Sulphonamide 1,4-dithia-7-azaspiro[4,4]nonane derivatives as gelatinase A inhibitors. *Bioorg. Med. Chem.* 21 (2013) 7752–7762.
- [33] L. Shi, H. Zhou, J. Wu, X. Li, Advances in the chemistry of quinoxalinone derivatives. *Mini Rev. Org. Chem.* 12 (2015) 96–112.
- [34] X. Li, J. Wang, L. Zhang, W. Xu, Design, synthesis and preliminary activity evaluation of novel peptidomimetics as aminopeptidase N/CD13 inhibitors. *Arch. Pharm. Chem. Life Sci.* 344 (2011) 494–504.
- [35] Y. Li, J. Zhang, W. Xu, H. Zhu, X. Li, Novel matrix metalloproteinase inhibitors derived from quinoxalinone scaffold (Part I). *Bioorg. Med. Chem.* 18 (2010) 1516–1525.
- [36] X. Li, J. Wang, J. Li, J. Wu, Y. Li, H. Zhu, R. Fan, W. Xu, Novel aminopeptidase N inhibitors derived from antineoplaston AS2-5 (Part I). *Bioorg. Med. Chem.* 17 (2009) 3053–3060.
- [37] X. Li, Y. Wang, J. Wu, Y. Li, Q. Wang, W. Xu, Novel aminopeptidase N inhibitors derived from antineoplaston AS2-5 (Part II). *Bioorg. Med. Chem.* 17 (2009) 3061–3071.
- [38] H. Yuan, X. Li, X. Qu, L. Sun, W. Xu, W. Tang, Synthesis and primary evaluation of quinoxalinone derivatives as potent modulators of multidrug resistance. *Med. Chem. Res.* 18 (2009) 671–682.

- [39] B. Desany, Z. Zhang, Bioinformatics and cancer target discovery. *Drug Discov. Today*. 9 (2004) 795–802.
- [40] X. Li, D. Wang, J. Wu, W. Xu, Novel approach to 3-methyl-1H-quinoxalin-2-ones. *Syn. Commun.* 35 (2005) 2553–2560.
- [41] A.C. Porter, Depletion and mutation of of topoisomerase II in animal cells. *Methods Mol. Biol.* 582 (2009) 245–263.
- [42] L. Shi, Q. Wang, H. Wang, H. Zhou, Y. Li, X. Li, Sulphonamide 1,4-dithia-7-azaspiro[4,4]nonane derivatives as gelatinase A inhibitors. *Bioorg. Med. Chem.* 21 (2013) 7752–7762.
- [43] X. Li, Y. Li, W. Xu, Design, synthesis and evaluation of novel galloyl pyrrolidine derivatives as potential anti-tumor agents. *Bioorg. Med. Chem.* 14 (2006) 1287–1293.
- [44] B.L. Yao, Y.W. Mai, S.B. Chen, H.T. Xie, P.F. Yao, T.M. Ou, J.H. Tan, H.G. Wang, D. Li, S.L. Huang, L.Q. Gu, Z.S. Huang, Design, synthesis and biological evaluation of novel 7-alkylamino substituted benzo[a]phenazin derivatives as dual topoisomerase I/II inhibitors. *Eur. J. Med. Chem.* 92 (2015) 540–553.
- [45] H. Wei, A.J. Ruthenburg, S.K. Bechis, G.L. Verdine, Nucleotide-dependent domain movement in the ATPase domain of a human type II DNA topoisomerase. *J. Biol. Chem.* 280 (2005) 37041–37047.
- [46] B. Pogorelčnik, M. Brvar, I. Zajc, M. Filipič, T. Solmajer, A. Perdih, Monocyclic 4-amino-6-(phenylamino)-1,3,5-triazines as inhibitors of human DNA topoisomerase II α . *Bioorg. Med. Chem. Lett.* 24 (2014) 5762–5768.

Highlights

- Quinoxaline peptidomimetic analogues derived from XK469 were proposed and many of them gave improved efficacies than the prototype.
- These derivatives tend to have similar mechanism of action with XK469.
- Molecular docking studies provided visual evidences of binding modes of target compounds.
- Two compounds stood out from bioevaluation and might be promising leads for further chemical optimization.